A Review of Galvanically Isolated Impedance-Source DC–DC Converters

Andrii Chub, *Student Member, IEEE*, Dmitri Vinnikov, *Senior Member, IEEE*, Frede Blaabjerg, *Fellow, IEEE*, and Fang Zheng Peng, *Fellow, IEEE*

***Abstract*—Impedance-source converters, an emerging technology in electric energy conversion, overcome limitations of conventional solutions by the use of specific impedance-source networks. Focus of this paper is on the topologies of galvanically isolated impedance-source dc–dc converters. These converters are particularly appropriate for distributed generation systems with renewable or alternative energy sources, which require input voltage and load regulation in a wide range. We review here the basic topologies for researchers and engineers, and classify all the topologies of the impedance-source galvanically isolated dc–dc converters according to the element that transfers energy from the input to the output: a transformer, a coupled inductor, or their combination. This classification reveals advantages and disadvantages, as well as a wide space for further research. This paper also outlines the most promising research directions in this field.**

***Index Terms*—DC–DC power converters, galvanic isolation, impedance-source (IS) converters, renewable energy sources.**

I. Introduction

RESEARCH in the field of impedance-source converters (ISCs) was initiated by the invention of the Z-source (ZS) inverter based on the ZS network [1]. ZS inverters (ZSIs) are able to provide buck–boost functionality by the single switching stage and improved reliability due to the inherent short-circuit immunity. These advantages urge active research in the field of impedance-source inverters. Recent ten years have seen a growing number of studies published in this area. The impedance-source (IS) technology was applied to all four basic converter types: dc–dc, ac–ac, dc–ac, and ac–dc. IS converters are applied in a very broad area from modern energy generation systems (renewable and alternative) to dc circuit breakers and electronic loads [2]. Impedance-source network (ISN) is the key element of any converter in this group. It consists of inductors, capacitors, and diodes (or switches). Any basic ISN can be represented as a two-port network that allows improved reliability, dc voltage (or current) gain, and provides immunity to shoot-through and open states. A number of novel ISNs have been proposed to improve the performance, cost, and reliability of IS converters [2].

A wide penetration of energy sources with low output voltage, like PV panels or fuel cells, has stimulated research into isolated step-up dc–dc converters with a wide input voltage variation range. They are intended to integrate low-voltage energy sources to the common dc link with much higher operating voltage. In this case, a magnetic element is used not only for galvanic isolation but also to define the dc gain range. Input voltage variations can be compensated at the controlled step-up stage inside the converter. The dc gain of this step-up stage is usually within the range from one to three. This range is selected to keep the efficiency of the controlled step-up stage within an acceptable range, while a major voltage step-up may occur at the isolation magnetic element with high efficiency.

The IS galvanically isolated dc–dc converters were reported as a suitable solution to interface low-voltage renewable or alternative energy sources [2], [3]. They have a wide input voltage and load regulation range that allows a better use of the energy source. Other advantages of the IS galvanically isolated dc–dc converters include the possibility of converterless integration of the short-term energy-storages (batteries) [4], bidirectional operation capability [5]–[7], and the inherent short-circuit protection. Converterless energy storage integration could be provided through direct connection of a battery in parallel with an ISN capacitor [8]. However, an additional bidirectional converter [9] can be used to enhance the operation range of the converter.

The aim of this paper is to review and systematize the state-of-the-art IS galvanically isolated dc–dc converters to fill the gap in the classification proposed in [2]. Section II presents a generalized comparison of the ISC technology with the voltage-source convertors (VSC) and current-source converters (CSC). Next, developments in the research of the IS galvanically isolated dc–dc converters are outlined. Then, the emerged IS galvanically isolated dc–dc converters, which have several hierarchical levels, are classified and their possible future research directions are indicated.

II. General Comparison With Voltage-Source and Current-Source DC–DC Converters

In contrast to the classical voltage-source and current-source converters (VSC and CSC, correspondingly), the ISC features an alternative power conversion approach, which combines both the advantages of the VSC and CSC and offers some extra benefits. This section explains the essence of the IS galvanically

Manuscript received December 10, 2014; revised March 11, 2015 and May 19, 2015; accepted June 18, 2015. Date of publication July 7, 2015; date of current version November 30, 2015. This work was supported by the Estonian Ministry of Education and Research (Project SF0140016s11) and by the Estonian Research Council under Grant PUT744. Recommended for publication by Associate Editor D. O. Neacsu.

A. Chub and D. Vinnikov are with the Department of Electrical Engineering, Tallinn University of Technology, Tallinn 19086, Estonia (e-mail: andrii.chub@ieee.org; dmitri.vinnikov@ieee.org).

F. Blaabjerg is with the Department of Energy Technology, Aalborg University, Aalborg 9220, Denmark (e-mail: fbl@et.aau.dk).

F. Z. Peng is with the Department of Electrical and Computer Engineering, Michigan State University, East Lansing, MI 48824 USA (e-mail: fzpeng@egr.msu.edu).

Color versions of one or more of the figures in this paper are available online at http://ieeexplore.ieee.org.

Digital Object Identifier 10.1109/TPEL.2015.2453128

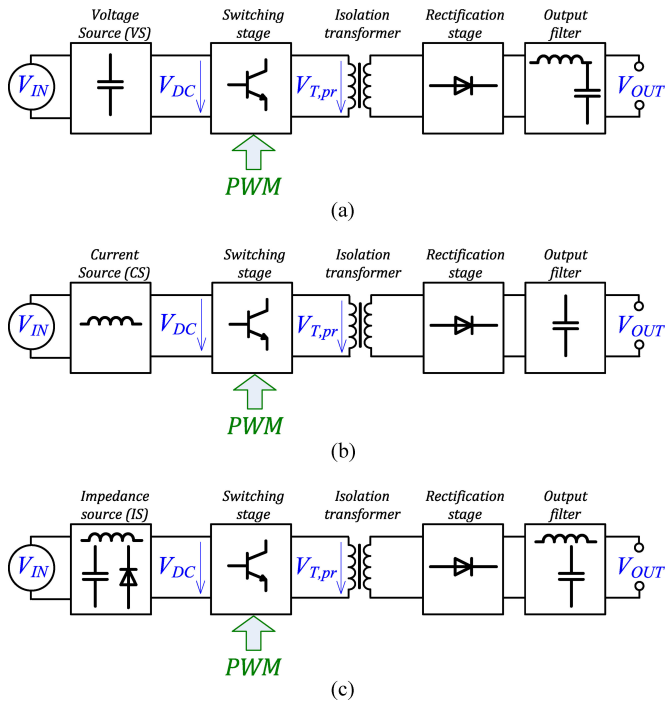

Fig. 1. Generalized block diagrams of (a) voltage-source, (b) CS, and (c) IS galvanically isolated dc–dc converters.

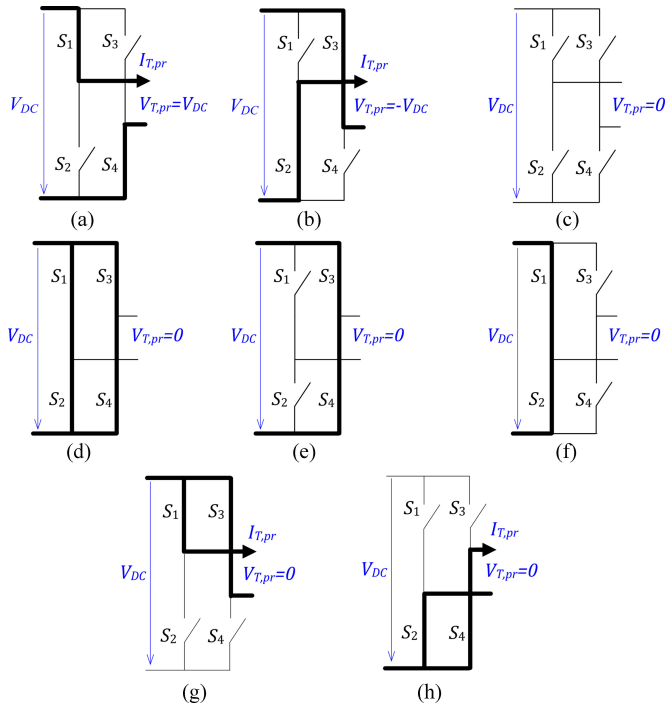

Fig. 2. Typical switching states of the single-phase inverter: (a) and (b) two active states, (c) one unstable state $V_{T,\mathrm{pr}} < V_{\mathrm{DC}}$, (d)–(f) three shoot-through states, and (g) and (h) two zero states.

isolated dc–dc converters in brief and compares them in general terms with the VSC and the CSC.

The generalized block diagrams of the three approaches are shown in Fig. 1. To simplify the discussion, the switching stage is represented by the single-phase full-bridge inverter followed by the isolation transformer and the diode rectifier with an output filter. Thereby, the inverter is controlled by a symmetrical pulse width modulation (PWM) [10].

The traditional VSC [see Fig. 1(a)] performs only the buck function of the input voltage by the variation of the duty cycle of the primary inverter switches. The VSCs are typically equipped with the output *LC* filter, which has an averaging effect on the applied pulsating voltage. In the traditional (square wave) PWM control, the duty cycle of the switches in the inverter bridge could vary between 0 and 0.5, thus providing minimum and maximum output voltage of the converter, correspondingly. Therefore, the switching period of the VSC typically consists of the combination of the active states [see Fig. 2(a) and (b)] and zero states [see Fig. 2(g) and (h)]. Since the VSC has the capacitive energy-storage element, it is very sensitive to the cross conduction of the switches in the inverter legs. Such short-circuit can easily destroy the converter; therefore, a dead time is typically introduced to eliminate the possibility of cross conduction at the duty cycles close to their maximum. Resulting from its simple realization and control, in the galvanically isolated dc–dc power conversion, the VSC is the most popular recent approach.

The CSC [see Fig. 1(b)] is characterized by the presence of the inductive storage element, which forms a current source (CS) on the dc side. In contrast to the VSC, the primary side of the CS galvanically isolated dc–dc converters performs the boost function only, i.e., the amplitude value of $V_{T,\mathrm{pr}}$ [see Fig. 1(b)] will always be higher than the input voltage. Therefore, shoot-through [see Fig. 2(d)–(f)] and active states [see Fig. 2(a) and (b)] are combined in the control of the primary inverter, and the duty cycle of inverter switches is typically higher than 0.5. The CS inverters have no open-circuit immunity, which means that at every time instant at least one loop with two devices conducting has to be ensured. Similarly to the VSC, the CS galvanically isolated dc–dc converters can be used in the bidirectional applications without significant hardware modifications. In the bidirectional power flow, the input inductor behaves as a first-order low-pass filter, thus suppressing the high-frequency ripple.

Since the VSC and CSC can realize either a buck or a boost function, an additional switching stage is necessary to widen the input voltage regulation range of these converters. For example, in renewable energy applications with widely changing input voltage, the VS galvanically isolated dc–dc converter is typically equipped with a boost converter (BC).

Traditionally, the BC is implemented before the main VSC [11]. In some cases, the BC is integrated in the secondary stage of the main VSC [12]. A similar approach can be adopted for the CSC, where the buck functionality is realized by the help of the additional step-down converter.

The ISC combines the main properties of the VSC and CSC, allowing both the buck and boost functions within the single switching stage. The ISN can be short- or open-circuited without any damages of the dc–dc converter. Therefore, all switching states illustrated in Fig. 2 can be realized with the ISC. Depending on the application, the ISC can be built either with a capacitive or an *LC* output filter [13]. As with the VSC and the CSC, the IS isolated dc–dc converter assures a bidirectional

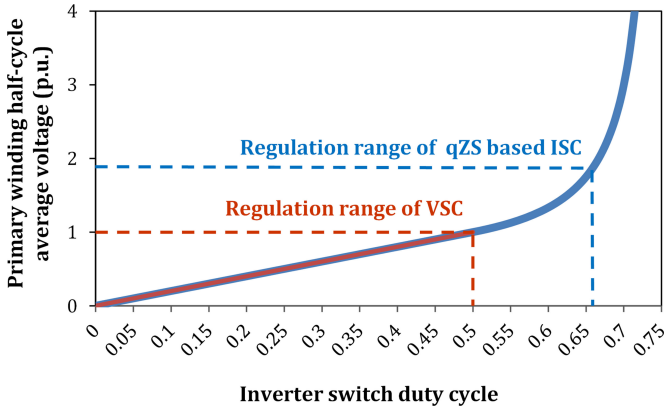

Fig. 3. Half-cycle average voltage of the primary winding of the isolation transformer as a function of the inverter switch duty cycle for the qZS-based ISC and the VSC.

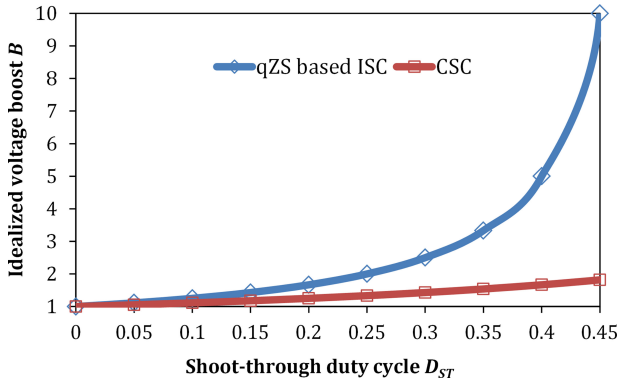

Fig. 4. Idealized voltage boost factor B as a function of the shoot-through duty cycle D_{ST} for the qZS-based ISC and the CSC.

power flow if the diode of the ISN is replaced by a bidirectionally conducting unidirectionally blocking switch. During the reversed power flow, the ISN operates as a low-pass filter and suppresses the high-frequency ripple without any reconfigurations [5]. Therefore, it justifies the ISC regarded as a versatile topology for applications in which a wide range of input voltage and load regulation is essential.

Fig. 3 shows a possibility of extending the regulation range for the traditional VSC by the use of the quasi-Z-source (qZS) network and a modified control algorithm [10]. Since it was assumed that the VSC has an output *LC* filter, the half-cycle average voltage values of the primary winding of the isolation transformer referred to the input voltage are compared for both approaches. For the qZS-based ISC, the operation duty cycle of the inverter switches can be theoretically extended from 0.5 to 0.75. However, in practical applications, the duty cycle values higher than 0.65 are not commonly recommended since they will lead to high conduction losses and a drastic decrease in the efficiency of the converter [14]. Hence, the ISC has nearly twice wider input voltage regulation range than that of the VSC.

With regard to its operation principle, the ISC is quite similar to the CSC, since both of them use the shoot-through switching states to step up the input voltage. In both approaches, the amplitude voltage of the primary winding of the isolation transformer ($V_{T,\mathrm{pr(peak)}}$) depends on the shoot-through duty cycle D_{ST}

$$D_{\mathrm{ST}} = \frac{t_{\mathrm{ST}}}{T} \tag{1}$$

where t_{ST} is the cross conduction time of the switches in the inverter bridge and T is the switching period. The idealized voltage boost across the inverter bridge in the qZS-based ISC is [15]

$$B_{\mathrm{qZS-ISC}} = \frac{V_{T,\mathrm{pr(peak)}}}{V_{\mathrm{IN}}} = \frac{1}{1 - 2 \cdot D_{\mathrm{ST}}}. \tag{2}$$

In the case of the CSC, the idealized voltage boost is [16]

$$B_{\mathrm{CSC}} = \frac{V_{T,\mathrm{pr(peak)}}}{V_{\mathrm{IN}}} = \frac{1}{1 - D_{\mathrm{ST}}}. \tag{3}$$

Results from the comparison of idealized voltage boost properties show that the voltage step-up capability of the ISC for the same shoot-through duty cycle D_{ST} is higher than that of the CSC (see Fig. 4). The twofold input voltage gain typical of the power conditioners for renewable energy sources is obtained with D_{ST} equal to 0.25 and 0.5 for the qZS-based ISC and the CSC, respectively. Since the duty cycles of the shoot-through and active states are interdependent in both topologies ($D_A = 1 - D_{\mathrm{ST}}$), this will result in higher RMS current in the isolation transformer of the CSC for the same operating conditions due to a shorter active state duty cycle D_A, which is used for transfer of the same amount of energy as in the ISC. Moreover, the ISCs have a narrower regulation range of the shoot-through duty cycle. The energy transfer in the boost mode during the active state is never less than half of the switching period. It leads to a better transformer utilization and absence of short current pulses with high amplitude, which is quite common for the CSCs regulated in a wide range. The input voltage gain of the ISC can be further improved by the cascading of the ISNs [17].

Since the operating principles are similar, the CSC faces a disadvantage of inductive overvoltages across the inverter bridge, which may lead to additional clamping circuits to be applied [18], [19]. Another issue of the CSC, the inrush current during the start-up at low output voltage, requires auxiliary start-up circuits to be implemented [20]. As a result, the introduction of these necessary auxiliary circuits significantly increases the complexity of the CSC, which finally makes it less attractive than the ISC.

Resulting from the discussion above, the main properties of the VSC, CSC, and ISC are compared in Table I. If properly implemented, the ISC may provide significant benefits over the two traditional isolated dc–dc power conversion approaches because of its regulation flexibility, power circuit versatility, and inherent reliability. On the other hand, in contrast to the popular VSC approach, the ISN will lead to higher complexity and to challenges related to efficiency, which is crucial for commercial success of the ISC technology.

TABLE I
COMPARISON OF MAIN PROPERTIES OF THE VSC, CSC, AND ISC

Property	VSC	CSC	ISC
Voltage boost	No	Yes	Yes
Voltage buck	Yes	No	Yes
Short-circuit immunity	No	Yes	Yes
Open-circuit immunity	Yes	No	Yes
Energy-storage element	One capacitor	One inductor	At least one capacitor and one inductor
Cascading of energy-storage elements	No	No	Yes
Realization and control simplicity	Simple	Complicated	Moderate

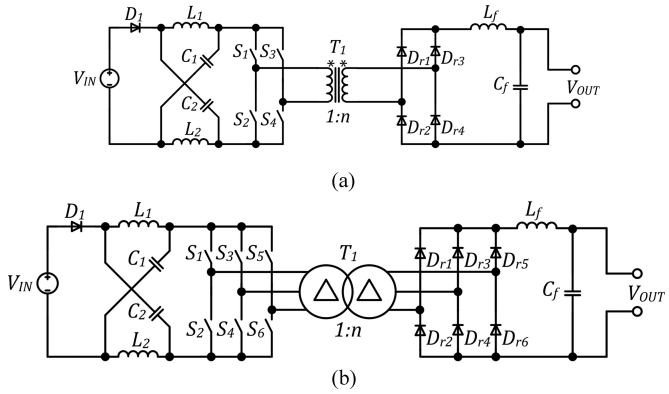

Fig. 5. State-of-the-art (a) ZSI-based single-phase and (b) three-phase galvanically isolated dc–dc converters [13], [21].

III. DEVELOPMENT OF THE IS GALVANICALLY ISOLATED DC–DC CONVERTERS

A. First Topologies

Originally, the ISC topologies can be broadly categorized as voltage fed or current fed. In terms of their simple practical realization and control, in a majority of applications, the voltage-fed approach is most popular today. The first voltage-fed IS-based galvanically isolated dc–dc converter [see Fig. 5(a)] reported in 2009 was derived from the classical voltage-source full-bridge isolated dc–dc converter by adding a ZS network to its input terminals [13]. Further improvement of the topology [see Fig. 5(b)] was connected with the modification in the intermediate high-frequency ac link, where the single-phase transformer was replaced by a three-phase one to achieve a higher power density [21]. These topologies were intended for the grid integration of low-voltage high-current fuel cells with rated power up to 10 kW.

The first IS galvanically isolated dc–dc converters presented in Fig. 5 were based on the voltage-fed ZSI; therefore, they suffered from the discontinuous input current during the shoot-through operation mode. Further progress on the IS galvanically isolated dc–dc converters was achieved by the introduction of the qZS network, which ensured a continuous input current [22]. Special shoot-through control methods used with the parasitic elements of the power circuit have led to the soft-switching qZS dc–dc converter [23].

B. Recent Development Trends

Focus today is on the efficiency and power density optimization of the IS dc–dc converters. A shift to resonant bridge with series resonant (SR) circuit, which utilizes the leakage inductance of the transformer, was proposed in [24]. This allows a considerable reduction of losses leading to a switching frequency rise and power density improvement.

Another possibility is synchronous rectification in the ISN. Preliminary results reported in [25] show the reduction of the losses in the qZS network by replacing the qZS diode with the MOSFET. It allows an efficiency rise by 2% within the qZS network. Active rectification is also possible at the voltage doubler rectifier (VDR) side. If all semiconductor components within the converter are active (e.g., MOSFETs), higher efficiency both in the VDR and IS stages as well as the controllable bidirectional operation can be achieved [26]. However, synchronous rectification requires more switches and driving circuits, as well as a complex control system with dead time implementation to avoid short-circuits [27].

New materials use is a popular trend in the modern power electronics industry. New magnetic materials can reduce the size of the ISN. Also, the new widebandgap semiconductors, like SiC and GaN, allow further loss reduction along with the switching frequency rise. GaN MOSFETs have shown good performance at the low voltage side in the PV microconverters [28]–[32]. Their utilization allows higher switching frequency; however, attention should be paid to the gate driver design and minimization of parasitic elements of the power circuit [33]–[35]. As modern SiC MOSFETs have proved their performance in high-voltage applications [36]–[40], they can be used in the synchronized VDR on the high voltage side. An appropriate selection of new widebandgap semiconductors and analysis of the benefits achieved along with economic concerns require additional research and development of new design guidelines.

C. Status of Progress

Since 2009, a number of new topologies of the IS galvanically isolated dc–dc converters have appeared, which can broadly be classified into three main groups according to the component which transfers energy from the input to the output side:

1) transformer based;
2) coupled inductor based;
3) with combined energy transfer.

The classification (see Fig. 6) is based on the operation mode of the component (components) that transfers energy from the input to the output side. In this paper, the transformer is any magnetic element that has two or more windings and operates with zero average core flux. Typical wave shapes of voltage across the winding and the core flux are shown in Fig. 7(a). During the energy transfer, the constant voltage is applied to a winding and the flux is changing with a slope that depends on the winding voltage amplitude and magnetizing inductance reflected to the same winding. Fig. 7(a) shows symmetrical

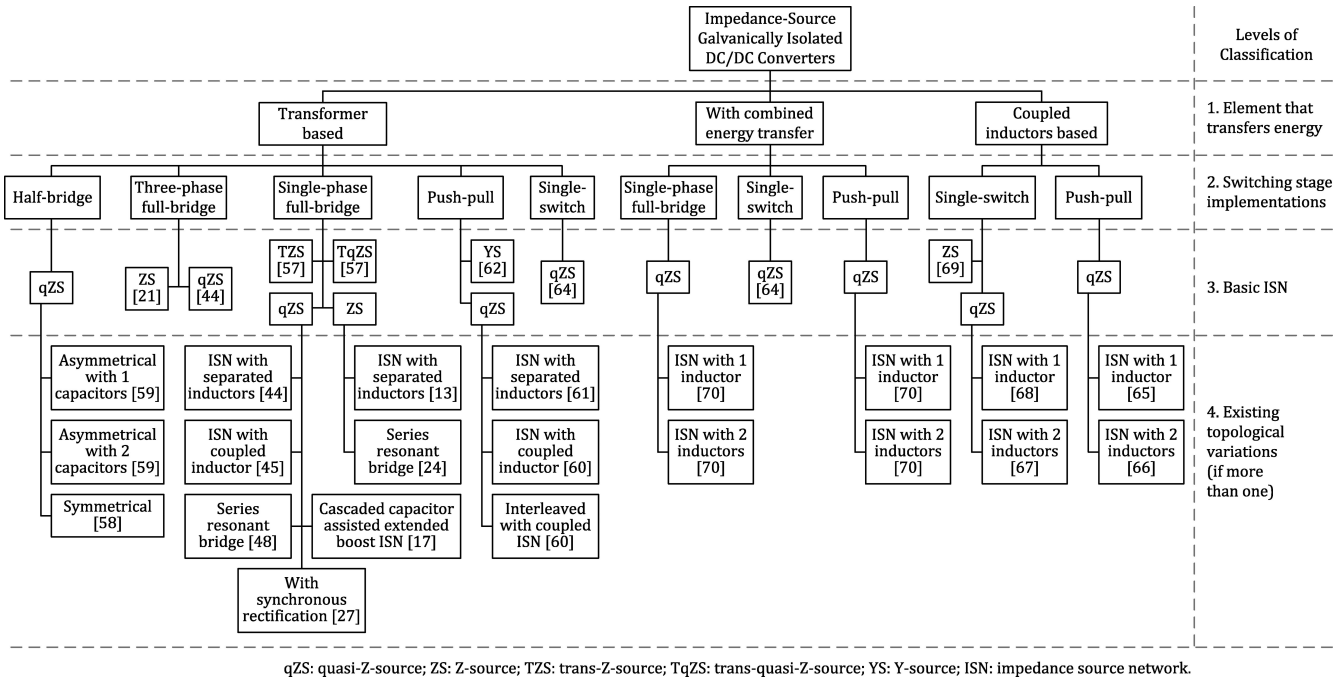

Fig. 6. Classification of the state-of-the-art IS galvanically isolated dc–dc converters.

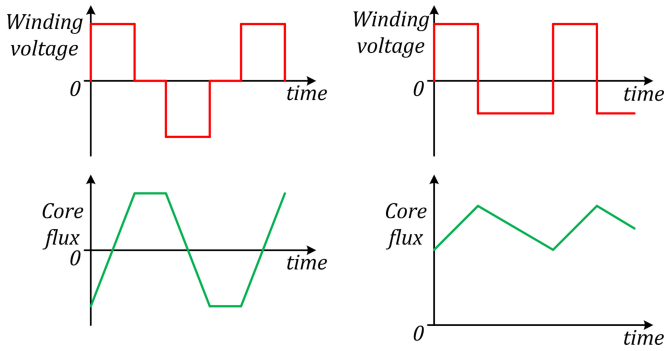

Fig. 7. Typical wave shapes of the winding voltage and core flux of: (a) transformer and (b) coupled inductor.

voltage pulses, even though they can also be asymmetrical. In this case, the volt–second balance as well as the zero average flux in the core must be maintained.

The term "coupled inductor" refers to a magnetic component with several windings and nonzero average core flux. The main difference of the coupled inductor and the transformer is in its functionality—a coupled inductor permanently stores a substantial amount of energy in the core. Fig. 7(b) shows an example of the voltage across the winding and the core flux of the coupled inductor. In a steady state, the volt–second balance must be maintained, while the voltage can either be symmetrical or asymmetrical.

The distinctive features of magnetically coupled elements are well known [41]. Despite superficial similarities between transformers and coupled inductors, these elements operate in different modes. Their construction is also different. The transformers are usually compact since the air gap in the core is small, or they are produced without it, to withstand the small unbalance of the core during regulation. Coupled inductors have to be designed with an air gap to ensure high average rated flux. Also, they are bulky and have higher leakage inductances than the transformers.

In the transformer-based IS dc–dc converters, the transformer transfers energy and ensures isolation, while inductors of the ISN only store the energy. In the coupled-inductor-based IS dc–dc converters, the coupled inductor(s) is usually a part of the ISN, and it serves not only for the energy transfer but also for the energy storage. The IS isolated dc–dc converters with combined energy transfer use both types of magnetically coupled components for energy transfer from the input to the output side.

IV. Transformer-Based IS Galvanically Isolated DC–DC Converters

This class of the ISC contains topologies that use a transformer for galvanic isolation and energy transfer. They can be divided into five basic groups:

1) with single-phase full-bridge switching stage;
2) with three-phase full-bridge switching stage;
3) with half-bridge switching stage;
4) with push–pull switching stage; and
5) with a single switch.

The first two categories can be merged into one with the full-bridge switching stage.

A. Converters With Full-Bridge Switching Stage

A generalized functional scheme for this group is shown in Fig. 8. The input part of the converter between the input terminals and the transformer is the basic structure of the IS inverter,

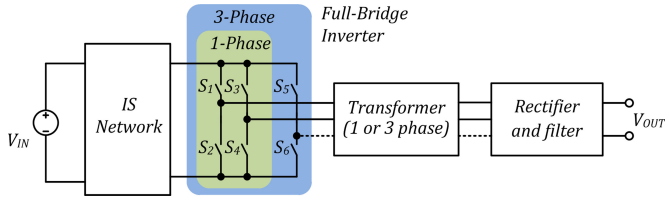

Fig. 8. Generalized functional scheme of the transformer-based IS galvanically isolated dc–dc converters with the full-bridge switching stage.

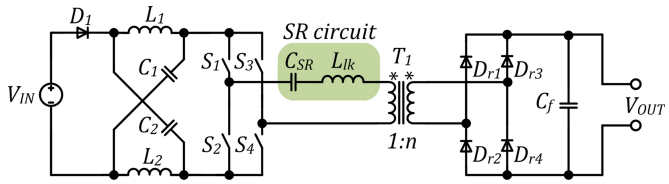

Fig. 9. ZS-based galvanically isolated SR full-bridge dc–dc converter [24].

which can have either one or three phases. These dc–dc converters consist of an IS inverter, a transformer, a rectifier, and a filter. The turns ratio n of the isolation transformer defines the range of the dc voltage gain. In this case, the ISN serves for adjusting the voltage across the transformer windings when the input voltage varies.

1) Z-Source: ZS-based converters utilize the ZS network that consists of two capacitors C_1, C_2, two inductors L_1, L_2, and a diode D_1 as shown in Fig. 5(a). The converter shown in the figure is historically the first in this group. It is based on the single-phase ZSI [13]. This converter has inherited advantages like buck–boost regulation and improved reliability and drawbacks like high component stress and discontinuous input current from the ZSI. The discontinuous input current substantially limits the application possibilities and performance of this converter. For example, it can be used with renewable energy sources, but it requires an additional filter at the input, which increases the system cost, volume, and failure rates. Also, bidirectional operation is possible in a symmetrical configuration [42], but it still has all the drawbacks of the ZSI, and the application range of such solutions is uncertain. The three-phase implementation of this converter is analyzed in [21]. In addition, an application with a distributed ZS network is discussed in [43].

The ZS-based converter with a single-phase full-bridge switching stage can easily use SR circuit in series with a transformer as shown in Fig. 9 [24]. The leakage inductance of the transformer could serve as a part of the resonance circuit, thus improving power density. In this case, the SR converter has a narrow regulation range in the frequency domain and improved buck–boost features. With the voltage buck–boost capability, the switching frequency range of ZS-based converter can be minimized to achieve higher efficiency over the entire input voltage and load variation. The converter still has a drawback of the circulating energy, while it is considerably minimized as compared to the conventional SR full-bridge converter. The reason is a narrower switching frequency regulation range. Another drawback lies in the discontinuous input current.

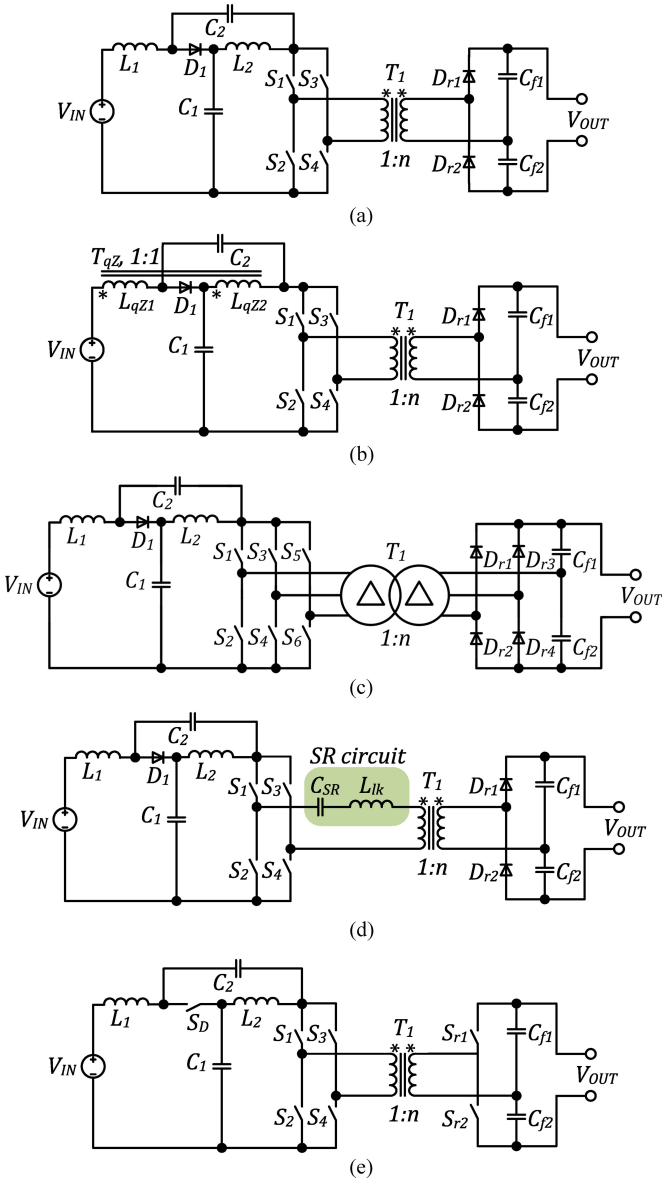

Fig. 10. qZS-based galvanically isolated full-bridge dc–dc converter with: (a) ISN with separated inductors [44], (b) ISN with coupled inductor [45], (c) with three-phase intermediate high-frequency ac link [44], (d) with SR bridge [48], and (e) with synchronous rectification [27].

2) Quasi-Z-Source: The quasi-Z-source inverter (qZSI) family was proposed in [15]. The qZSI has inherited all the advantages of the ZSI, but it has lower component stress and continuous input current. The single-phase and the three-phase qZS-based galvanically isolated dc–dc converters are proposed in [44]. Two implementations of the single-phase qZS-based ISC are shown in Fig. 10(a) and (b). In the first case, the qZS network contains the inductors L_1 and L_2 and capacitors C_1 and C_2. It is advisable to implement the qZS network with the single-coupled inductor T_{qz} [see Fig. 10(b)] in order to improve power density [45]. Advantages inherited from the qZSI make this converter a superior solution for modern distributed energy generation systems. Additional benefits are gained with the use of the VDR based on diodes D_{r1}, D_{r2} and capacitors

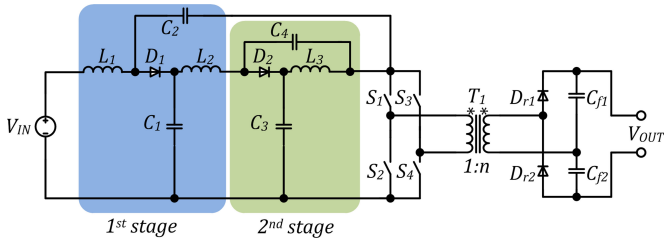

Fig. 11. Cascaded CAEB two-stage qZS-based galvanically isolated full-bridge dc–dc converter [17].

C_{f1}, C_{f2}. It is recommended to use the VDR for any step-up converter in the transformer-based group. It enables the use of the transformer with a reduced turns ratio n, which leads to lower transformer parasitic elements. The topology has demonstrated its good performance in the fuel cell applications and permanent magnet synchronous generator (PMSG)-based wind turbines [46], [47]. It is recommended to implement the topology with the three-phase intermediate high-frequency ac link [see Fig. 10(c)] for high-power applications [44].

The qZS-based galvanically isolated dc–dc converter has attracted attention of researcher because of the numerous advantages of the qZS network in power conversion. Several topological variations have been derived to further improve this topology. SR bridge to be used within this converter [see Fig. 10(d)] is proposed in [24] and discussed in [48]. Advantages of this converter are similar to those of the SR ZS converter (see Fig. 9), while it features continuous input current. When operating in the buck mode, the circulating energy could be an issue. Therefore, additional research and elaboration of detailed design guidelines are required. Also, the light-load operation may limit controllability as an inherent drawback of SR converters. Furthermore, the possible range of soft switching must be analyzed. Another possible improvement of the reference qZS-based full-bridge topology is the use of synchronous rectification. The improved topology with solely fully controlled switches shown in Fig. 10(e) allows more than 2% higher efficiency [27] because of minimized conduction losses in the qZS semiconductor element that is the major contributor of its losses [25], [49]. It can also provide the bidirectional operation without additional circuits. Moreover, the use of active VDR may result in a soft-switching operation, like in the dc–dc converters presented in [50]–[52]. Thus, additional research is required.

Another alternative to improve the qZS-based topology is to employ a cascaded qZS network. An inverter with the cascaded qZS network is proposed in [53] to further improve the step-up performance. Diode assisted and capacitor assisted families of cascaded qZS topologies have been analyzed.

Capacitor-assisted topologies have better voltage step-up performance and fewer semiconductor elements than those of the diode assisted. Therefore, the capacitor-assisted extended boost (CAEB) topologies were applied to the qZS-based galvanically isolated dc–dc converter in [17]. This topology with two qZS stages is shown in Fig. 11. Cascaded two-stage implementation of the qZS network contains two times more components and can provide a higher step-up than the ordinary qZS-based converter with the same shoot-through duty cycle. The purpose of the solution was to improve transformer utilization by narrowing the shoot-through duty cycle regulation range. In practice, additional components bring in losses and additional volume that cannot be compensated by the improvements in the transformer operation mode. The cascaded converter cannot overcome the simple qZS-based approach by its overall performance mostly due to the increased losses.

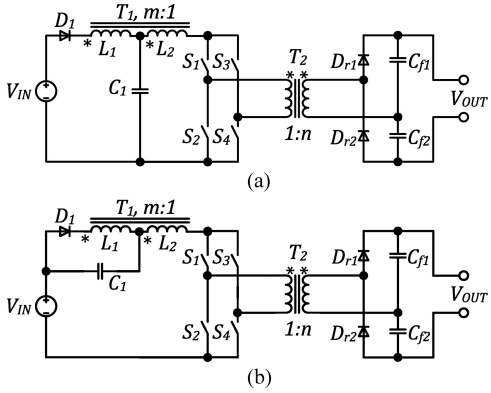

Fig. 12. (a) TZS-based and (b) TqZS-based galvanically isolated full-bridge dc–dc converters [57].

The review of the ISNs in [2] shows that only some ISNs can provide continuous input current, which is needed in most of the modern power electronics applications for distributed generation. The qZS network has a superior region of continuous input current. There are several ZS-based ISNs that have coupled inductors (with nonunity turns ratio), which influence the dc gain factor by their turns ratio m, for example: Γ-Z-source [54], trans-Z-source (TZS) [55], and Y-source (YS) [56]. They usually have discontinuous input current. Such converters have better step-up performance than the conventional ZS or qZS. In the case of the transformer-based IS galvanically isolated dc–dc converters, these networks allow dc voltage gain to be distributed between the transformer (defined by n) and the coupled inductor (defined by m). This leads to distributed parasitic elements and better switching performance.

3) Trans-Z-Source: TZS-based galvanically isolated dc–dc converter family was proposed in [57]. It consists of the TZS-based single-phase dc–dc converter and the trans-quasi-Z-source (TqZS)-based single-phase dc–dc converter shown in Fig. 12. Three-phase implementation can be easily derived from a single-phase design. In these converters, the dc voltage gain of TZS or TqZS networks depends not only on the shoot-through duty cycle but also on the turns ratio m of the coupled inductor T_1. The IS network contains fewer passive elements: one capacitor C_1, coupled-inductor T_1, and diode D_1. Both converters have discontinuous input current. Experimental verification has shown that the TqZS-based galvanically isolated dc–dc converter has lower start-up current than that of the TZS inverter based. In the future, it is required to establish the application range and detailed design guidelines of those converters.

B. Converters With Half-Bridge Switching Stage

In contrast to the full-bridge counterparts, the half-bridge IS galvanically isolated dc–dc converters feature a reduced number

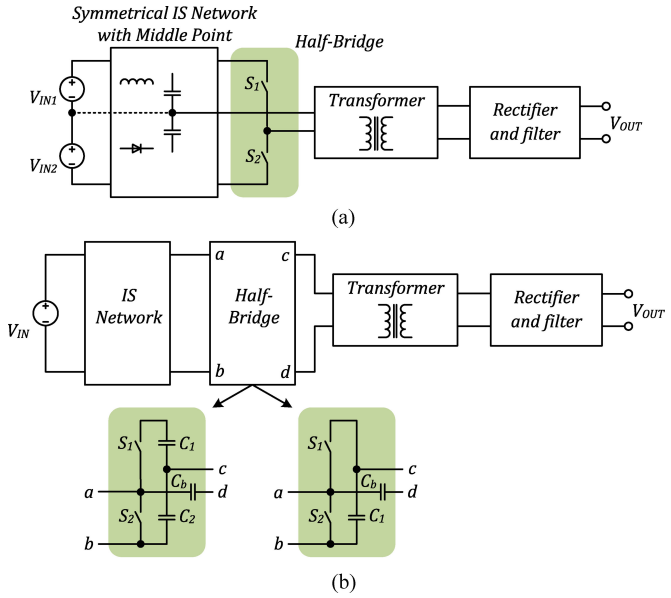

Fig. 13. Generalized functional schemes of the transformer-based IS galvanically isolated dc–dc converters with half-bridge switching stage: (a) symmetrical and (b) asymmetrical.

of switching elements. The IS galvanically isolated dc–dc converters with a half-bridge switching stage can be broadly classified into symmetrical and asymmetrical topologies. Symmetrical topologies [see Fig. 13(a)] require a symmetrical ISN structure, which must have a middle point. The half-bridge switching stage supplies a transformer with bipolar pulses of the same magnitude, and the dc blocking capacitor is generally avoided. Symmetrical converters can operate either with a single or two input voltage sources connected to the middle point of the ISN. The output voltage of the converter is controlled by the variation of the shoot-through duty cycle of the inverter similarly to the IS dc–dc converters with the full-bridge switching stage.

Asymmetrical converters can have the half-bridge switching stage of two types: with single or two capacitors [see Fig. 13(b)]. The high-side and the low-side transistors of the half-bridge inverter are driven complementary, and the dc blocking capacitor is typically required to prevent the possible saturation of the isolation transformer. The difference between the switching stages lies within the dc-link implementation and connection of the transformer to the dc link. The configuration with a single capacitor can be obtained from that with two capacitors if the top capacitor in the dc link is short circuited. The low-side transistor S_2 performs shoot-through states for dc voltage gain regulation on both types of the asymmetrical half-bridge IS galvanically isolated dc–dc converters.

1) Quasi-Z-Source: All the existing half-bridge IS galvanically isolated dc–dc converters are based on the qZS network. The symmetrical qZS half-bridge dc–dc converter (see Fig. 14) has two identical qZS networks with a neutral node *n* between the capacitors C_1 and C_3 [58]. Mirror connection of two qZSNs enables the symmetrical structure of the ISN. Each qZS network needs to handle half of the converter rated power. The voltage stress of the half-bridge switches equals the sum of the capacitor voltages on both qZS networks.

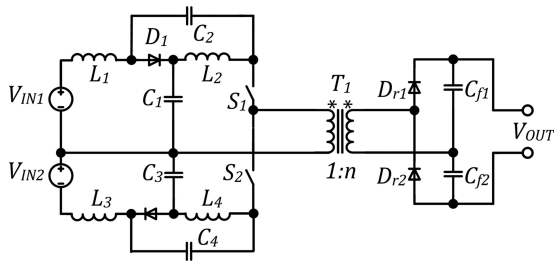

Fig. 14. qZS-based galvanically isolated symmetrical half-bridge dc–dc converter [58].

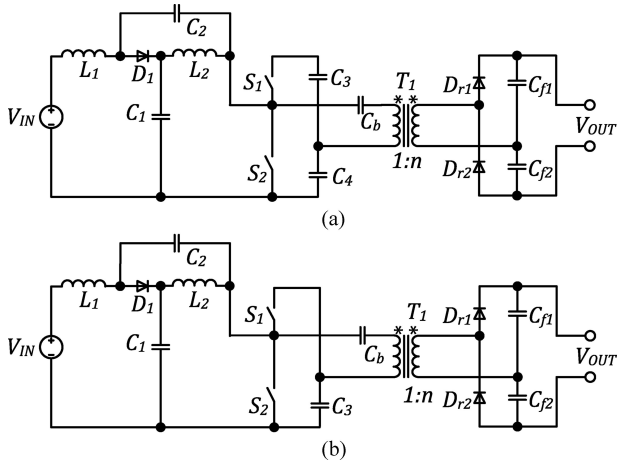

Fig. 15. qZS-based galvanically isolated asymmetrical half-bridge dc–dc converters: (a) with two capacitors and (b) with a single capacitor in the switching stage [59].

The half-bridge ISC can be simplified considerably by the implementation of the asymmetrical half-bridge concept (see Fig. 15) [59]. In that case, the high-side and the low-side switches of the half-bridge inverter are driven complimentary, and the energy is transferred through the isolation transformer TX by the asymmetrical pulses. It leads to unequal voltages across the VDR capacitors C_{f1} and C_{f2} [see Fig. 15(a)] and also requires the dc blocking capacitor C_b in series with the primary winding of the isolation transformer to prevent its possible saturation. If properly realized, the SR circuit formed by the dc blocking capacitor and primary winding leakage inductance of the isolation transformer could result in the soft switching of the half-bridge inverter switches.

The asymmetrical half-bridge topology can be simplified further by the reconfiguration of the switching stage as shown in Fig. 15(b). In general, the operating principle of the modified topology remains the same. Minimized component count will lead to higher voltage stress of the primary side capacitors C_3 and C_b. Therefore, the capacitor C_3 must be specified for the operating voltage equal to the amplitude value of the intermediate dc-link voltage. The blocking capacitor C_b needs to withstand higher dc voltage because the half-bridge switching stage supplies the transformer with unipolar voltage pulses in contrast to bipolar in the topology shown in Fig. 15(a).

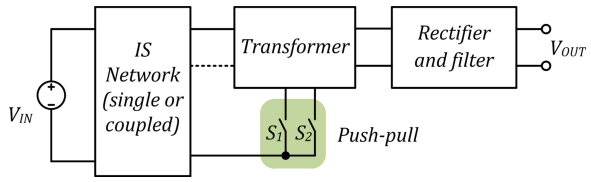

Fig. 16. Generalized functional scheme of the transformer-based IS galvanically isolated dc–dc converters with the push–pull switching stage.

In several cases, the qZS-based galvanically isolated asymmetrical half-bridge dc–dc converters can be considered as a cheaper alternative to the transformer-based ISC with a full-bridge switching stage. However, as compared to the full-bridge-based converter, the asymmetrical half-bridge topologies have only one shoot-through state per switching period. Therefore, the qZS network operates with the frequency equal to the switching frequency, and its passive components have double values as compared to those of the full-bridge counterpart.

C. Converters With Push–Pull Switching Stage

A generalized functional scheme of this group is shown in Fig. 16. This group has several advantages over the full-bridge-based converters, such as lower number of switches, simpler control, and lower conduction losses in low input voltage applications. However, the full-bridge counterparts can provide higher output power levels due to the higher number of switches. Usually, the switches work interleaved to improve the input current ripple.

1) Quasi-Z-Source: The qZS-fed push–pull converter (qZSFPPC) family has been proposed recently [60]. It is derived from the current-fed push–pull converter family by replacing the input inductor with the qZS network. Such family could be derived for almost any ISN, but almost none of them have continuous input current. This family includes the qZSFPPC and the interleaved qZS-fed push–pull converter (IqZSFPPC) that both are shown in Fig. 17. They have fewer switches than the full-bridge IS-based converters, while they provide similar performance.

The qZSFPPC [see Fig. 17(a)] employs a qZS network with a coupled inductor. It has the operation principle quite similar to that of the qZS-based full-bridge converter. The qZS-based galvanically isolated push–pull dc–dc converter with a separated inductor (see Fig. 18) is described in [61]. Its differences from the qZSFPPC lie in simpler implementation of the qZS network and worse utilization of the VDR. The IqZSFPPC [see Fig. 17(b)] contains a magnetically coupled qZS network, which can be represented as two qZS networks with full magnetic coupling within the coupled inductor T_{qZ}. In the IqZSFPPC, the leakage inductances of the coupled inductor define the input current ripple, while the magnetizing inductance defines the current ripple in the windings. This dependence implies a complicated design of the magnetic component for the IqZSFPPC.

The control principle of these converters is quite similar to the reference current-fed push–pull converter family except for the duty cycle regulation range, because of the improved voltage step-up performance. The leakage inductances are not taken into account in [60] and [61]. This means that, in practice, these converters will utilize active or passive clamping at the input side. Nevertheless, these converters are recommended for low input voltage and high input current applications because the input current loop contains only one power switch, which may assure lower conduction losses. The IqZSFPPC has more passive elements, but they are rated for lower current or voltage stress. Therefore, the final power densities of the noninterleaved and the interleaved converters can be close to each other.

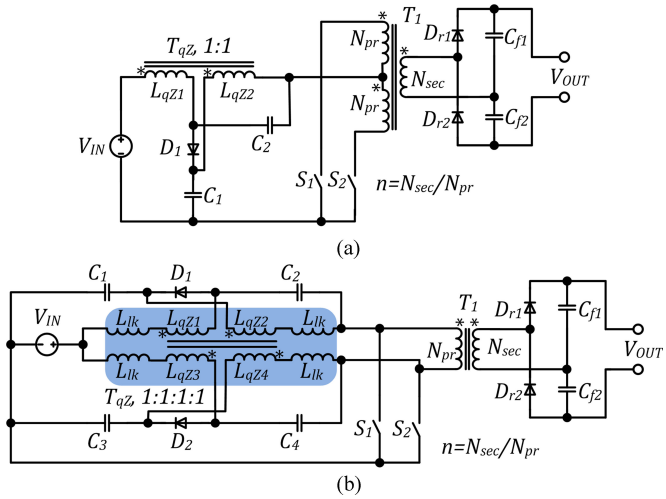

Fig. 17. qZSFPPC family [60]: (a) qZSFPPC with coupled inductors and (b) IqZSFPPC.

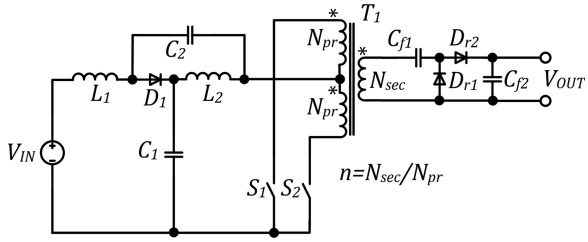

Fig. 18. qZS-based galvanically isolated push–pull dc–dc converter with separated inductors [61].

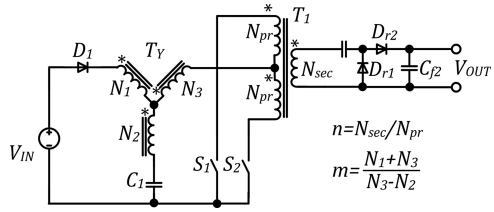

Fig. 19. YS-based galvanically isolated push–pull dc–dc converter [62].

2) Y-Source: Recent designs of IS converters are using the novel YS network [2]. A YS converter in the group of transformer-based IS galvanically isolated dc–dc converters with the push–pull switching stage is shown in Fig. 19 [62]. The YS network consists of the capacitor C_1, the coupled

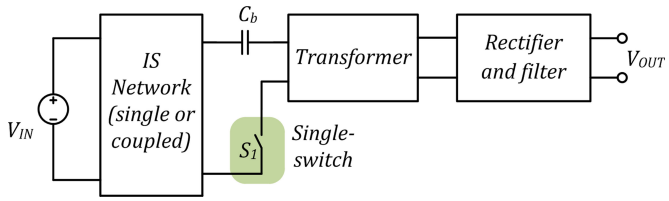

Fig. 20. Generalized functional scheme of the transformer-based galvanically isolated IS dc–dc converters with a single switch.

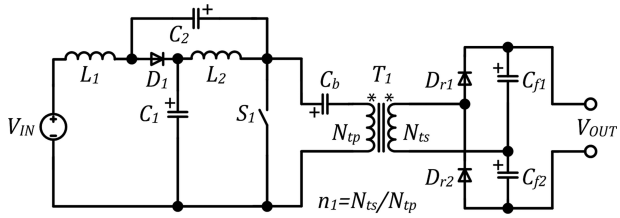

Fig. 21. qZS-based transformer-based IS galvanically isolated single-switch dc–dc converter [64].

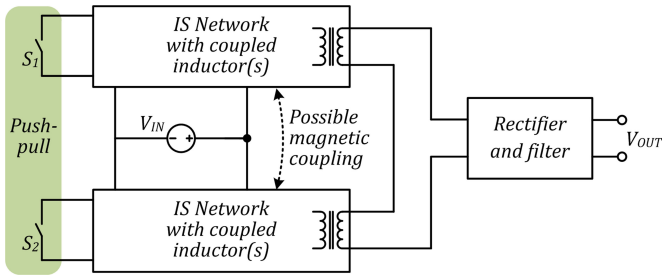

Fig. 22. Generalized functional scheme of the coupled-inductor-based galvanically isolated IS dc–dc converters with the push–pull switching stage.

inductor T_Y, and the diode D_1. That network is regarded under the group of IS networks with coupled inductors. In this case, the coupled inductor T_Y has three windings, which give some level of freedom during the design of this converter because the characteristic value *m* depends nonlinearly on the turns number of each winding. This value defines the step-up characteristic of the YS network. Also, the converter utilizes the Greinacher VDR, while the bridge VDR is commonly used and has slightly better performance [3].

According to the reports, the performance of the YS network converter is close to that of the TZS network. In addition, it suffers from voltage overshoots caused by the leakage inductances of the coupled inductor due to discontinuous input current [63] like other ISNs with a coupled inductor. Moreover, the three-winding coupled inductor is more complicated to design and more expensive than the two-winding inductor used in the TZS network. The closed-loop control of the YS-based converters and their application possibilities need comprehensive coverage. To compare the YS network with other ISNs with coupled inductors (TqZS, Γ-Z-source, etc.), analysis and experiments are required to evaluate practical application possibilities and overall performance of the YS network-based converters. From the sources available, it seems to have a good performance and versatility for inverters, while in dc–dc applications its advantages may be less apparent.

D. Converters With a Single Switch

A generalized functional scheme of this group is shown in Fig. 20. Simplest in the class of transformer-based converters, it has only one switch, and, thus, is intended for the low-power and low-voltage applications. Due to its simplicity, the ISN operates at the switching frequency of the switch. This group of converters has been proposed recently as a concept, and it needs further study to identify application possibilities and limitations imposed by the simplified switching stage.

1) Quasi-Z-Source: This group contains only one converter—the qZS-based single-switch IS converter shown in Fig. 21. Derived from a single-switch nonisolated qZS dc–dc converter [64], it comprises the qZS network, power switch S_1, isolation transformer T_1, dc blocking capacitor C_b, and VDR. Blocking capacitor is required to avoid saturation since the transformer is fed with unipolar voltage pulses. The power switch S_1 performs shoot-through states for the qZS network. The qZS network feeds the transformer T_1 with unipolar voltage pulses with varying magnitude and duty cycle. It results in unequal voltage over VDR capacitors C_{f1} and C_{f2}. Average value of the transformer input voltage is equal to the voltage across capacitor C_2, while the magnitude of the imaginary dc link is equal to the sum of qZS capacitors voltages. It means that VDR capacitors are charged to the values of the qZS capacitors voltages reflected to the output. Resonant soft switching could be achieved if the blocking capacitor is properly adjusted to form a SR circuit with the leakage inductance of the isolation transformer T_1. Advantages of that converter lie in low-power and low-voltage applications since it contains only one power switch. The switch can suffer from high current stress at a wide voltage regulation due to the short conduction state at the low dc voltage gain, since the topology requires nonzero switch duty cycle for normal operation. Additional research is required here.

V. Coupled-Inductor-Based IS Galvanically Isolated DC–DC Converters

This class of the ISC contains topologies that use a coupled inductor as a part of the ISN, as well as for the galvanic isolation and energy transfer from the input side to the output side. Those converters are not as numerous as the previous one. The first topology appeared in the literature at the beginning of 2012 [65]. During the last three years, several new converters from this class have been proposed. They can be divided into two main groups:

1) with push–pull switching stage;
2) with a single switch.

A. Converters With Push–Pull Switching Stage

This group consists of two push–pull-based converters that could be organized into one family based on the commonly used qZS network. A generalized functional scheme for this group is shown in Fig. 22.

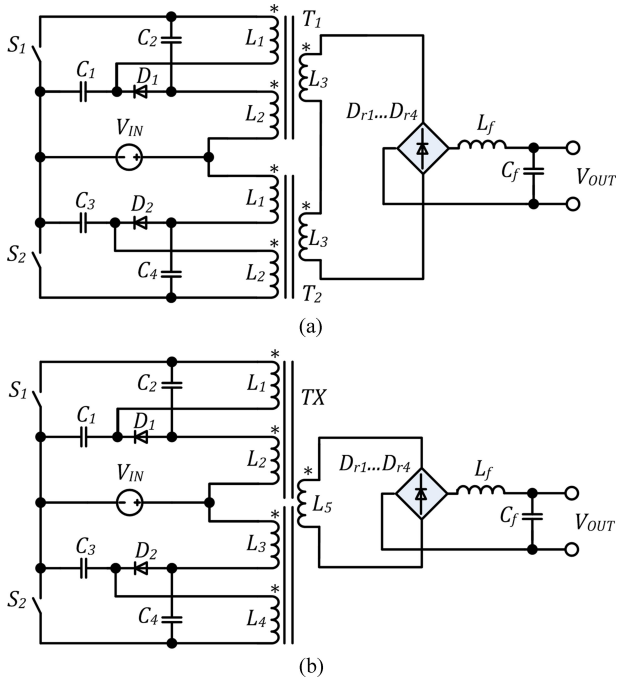

Fig. 23. qZS-based galvanically isolated push–pull dc–dc converters: (a) with two coupled inductors and (b) with a single-coupled inductor [65], [66].

1) Quasi-Z-Source: The qZS derived push–pull dc–dc converter with two coupled inductors is reported in [65] and analyzed in [66]. It consists of two qZS networks: C_1, C_2, T_1, D_1 and C_3, C_4, T_2, D_2 as shown in Fig. 23(a). Three-winding coupled inductors T_1 and T_2 provide galvanic isolation and store energy in the form of equivalent magnetizing current (i.e., flux through the core of the coupled inductors). The turn-on state of the transistors corresponds to the shoot-through behavior of the IS inverter. This converter shows good performance in wind power applications due to its wide feasible input voltage regulation range, especially for PMSG-based wind turbines. It can be also envisioned as two single-switch converters connected in parallel at the input and in series at the output, where they are sharing a common output rectifier and a filter. At low step-up, this converter transfers energy in the narrow pulses with high current amplitude, which is the main drawback that limits the practical regulation range. Flat efficiency curve at high switching frequency can be achieved in the "full-SiC" implementations [40].

Further improvement in the group of push–pull-based converters is possible through magnetic coupling of qZS networks [65]. Full coupling between T_1 and T_2 should be avoided because it leads to self-compensation of windings, and such converter is infeasible. Partial coupling is a good option that leads to a single-coupled inductor implementation of the push–pull-based topology. The qZS derived push–pull dc–dc converter with a single-coupled inductor is shown in Fig. 23(b). This topology reported in [65] looks promising, but neither studies of the design of the coupled inductor *TX* nor full design guidelines have been provided.

Both converters use a diode bridge rectifier with an output *LC* filter. These topologies require careful design to avoid high-voltage oscillation over the rectifier diodes and tertiary windings of the coupled inductors. They may appear in the topology with two-coupled inductors during the freewheeling state, when voltages across L_5 and L_6 compensate each other.

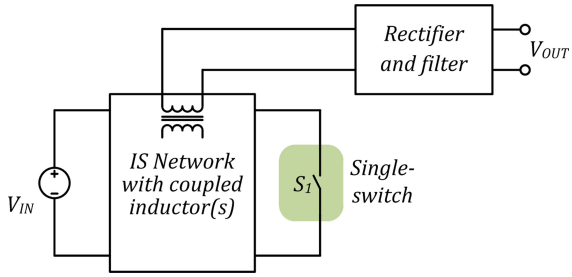

Fig. 24. Generalized functional scheme of the coupled-inductor-based galvanically isolated IS dc–dc converters with a single switch.

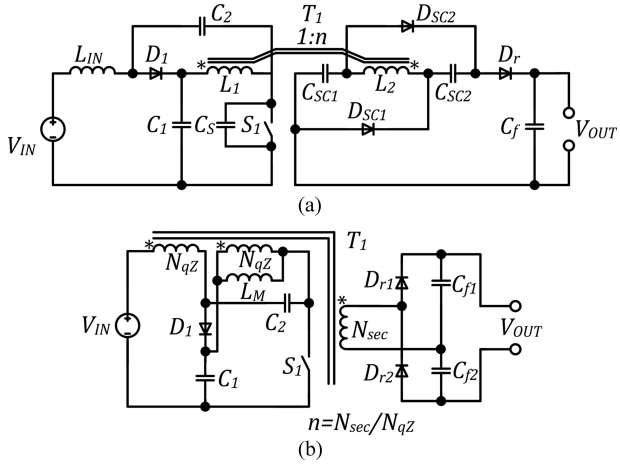

Fig. 25. qZS-based galvanically isolated coupled-inductor-based single-switch dc–dc converters: (a) with two inductors [67] and (b) with a single inductor [68].

B. Converters With a Single Switch

This group contains three recently proposed converters based on the typical qZS and ZS networks. A generalized functional scheme for this group is shown in Fig. 24.

1) Quasi-Z-Source: qZS-based single-switch converter with two inductors within the ISN has been reported in [67]. In the qZS network, the second inductor is replaced with a coupled inductor T_1 as shown in Fig. 25(a). The magnetizing inductance reflected to the primary winding serves as the part of the qZS network along with $L_{\rm IN}$ to store the energy. Inductor T_1 also provides galvanic isolation and energy transfer to the output. The output part contains the switched capacitor cell $D_{\rm SC1}$, $D_{\rm SC2}$, $C_{\rm SC1}$, $C_{\rm SC2}$ for additional voltage step-up and the rectifier D_r with the filter capacitor C_f. The output side utilizes leakage inductance of the coupled inductor as a part of the rectifier that limits the current ripple. The main advantage is that the output current ripple is reflected to the inductance L_1 in the qZS network, but does not influence the input current with low ripple. On the other hand, such implementations require two magnetic components.

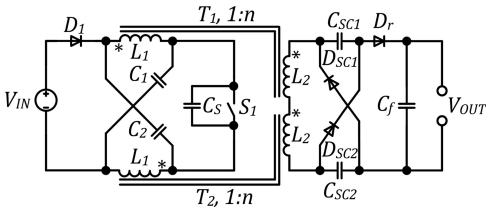

Fig. 26. ZS-based galvanically isolated single-switch dc–dc converter [69].

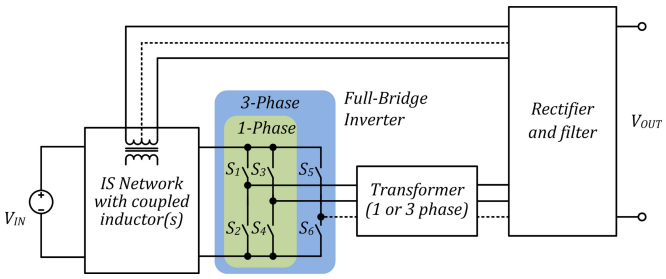

Fig. 27. Generalized functional scheme of the galvanically isolated full-bridge IS dc–dc converters with combined energy transfer.

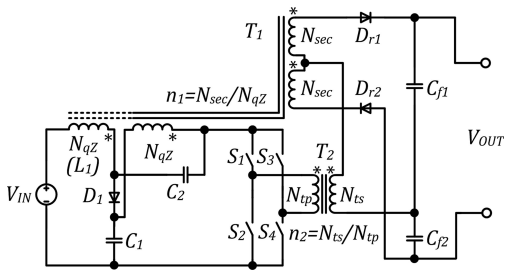

Fig. 28. qZS-based galvanically isolated full-bridge dc–dc converter with combined energy transfer [70].

Another single-switch qZS-based dc–dc converter shown in Fig. 25(b) has been derived from the qZS push–pull dc–dc converter with two coupled inductors [see Fig. 23(a)] [3], [68]. It contains only one magnetic component. In contrast to the previous qZS converter, this converter has continuous input current with higher ripple, because the reflected output current ripple is shared between the primary windings of the coupled inductor T_1. It also utilizes the bridge VDR, which provides continuous output capacitor current (only one of them charges simultaneously) and low component count. Here, the slight drawback with higher input current ripple can be neglected when the converter operates in a high step-up mode and couples the low and high voltage sides. This converter shows good performance in a wide input voltage range [68].

2) Z-Source: Another converter in this group was derived in the same manner as the qZS-based single-switch converter with two inductors [69]. Both inductors of the single-switch ZS isolated dc–dc converter are coupled to maintain a symmetrical structure of the ZS network as shown in Fig. 26. In contrast to the conventional ZS network, the current in the ZS inductors has higher ripple due to the reflection of the output current to the input side. The leakage inductance of secondary windings serves as a filter in the output side. The input current is discontinuous. As compared to single-switch qZS converters, this converter has higher stress of the elements. This topology can be improved by magnetic coupling of coupled inductors T_1 and T_2. Full coupling seems to be the best choice. In this case, the ZS network would be based on the three-winding coupled inductor that carries two times higher flux. The feasibility of such systems needs to be investigated with the VDR, which also seems to be a superior solution for the IS isolated dc–dc converters.

Coupled-inductor-based converters are more complicated to design than transformer-based converters. They have shown good performance in wind energy applications, where the input voltage varies most of all. This class of converters contains several topologies. Many novel topologies can be derived with other ISNs that have not been applied yet.

VI. IS Galvanically Isolated DC–DC Converters With Combined Energy Transfer

The latest trend of the ISCs is to use the combined energy transfer principle. Converters of this class contain coupled inductors and transformers, which allows magnetically coupled components to be used for energy transfer, and, thus, a better dc voltage gain is the result. Coupled inductors of the ISN contain additional winding(s) for energy transfer to the output side. Several secondary windings are connected to the rectifier and filter at the output side. They provide additional output voltage, and, thus, improve the voltage step-up operation of the ISC. First topologies were proposed in [70]. This class presents the same categories at the second level of classification as the transformer-based converters because of similar switching stages. All the converters reported in [64] and [70] are based on the qZS network and represent three basic groups:

1) with single-phase full-bridge switching stage;
2) with push–pull switching stage;
3) with a single switch.

This solution is versatile because the dc voltage gain and energy transfer distribution between the magnetic elements could be defined by two turns ratios.

A. Converters With Full-Bridge Switching Stage

This group of converters can be described by the generalized functional scheme shown in Fig. 27. The concept is based on the combination of the transformer-based converters with the full-bridge switching stage and a coupled-inductor-based converter with a single switch. Switching stage could be implemented using a single-phase and a three-phase configuration. The single-phase configuration seems to be simpler and more attractive in practice.

1) Quasi-Z-Source: The qZS ISC shown in Fig. 28 was proposed in [70]. The coupled-inductor T_1 in the qZS network contains two additional windings connected in series with the output winding of the isolation transformer T_2. Each secondary

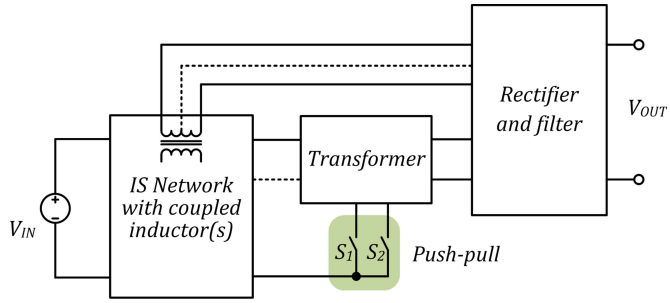

Fig. 29. Generalized functional schemes of the galvanically isolated IS push–pull dc–dc converters with combined energy transfer.

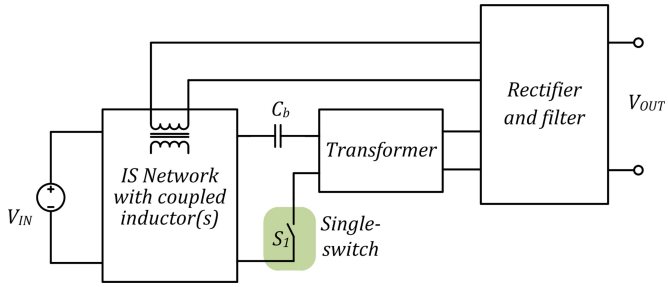

Fig. 31. Generalized functional scheme of the galvanically isolated IS single-switch dc–dc converters with combined energy transfer.

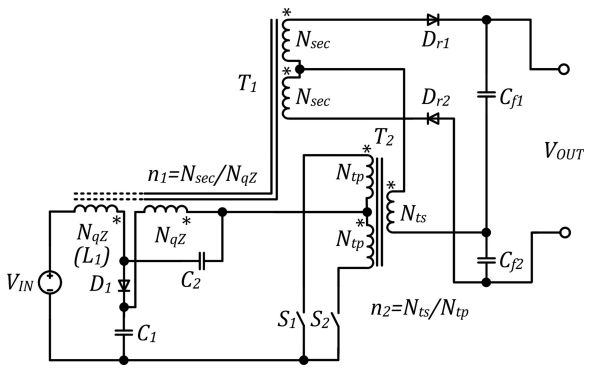

Fig. 30. qZS-based galvanically isolated push–pull dc–dc converter with combined energy transfer [70].

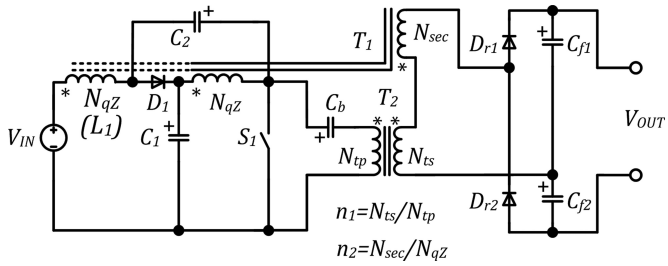

Fig. 32. qZS-based galvanically isolated single-switch dc–dc converter with combined energy transfer [64].

winding feeds the VDR together with the secondary winding of the transformer T_2 during active state in the inverter bridge. The proposed connection of the output windings allows the use of a single VDR. Filter capacitors are charged symmetrically. The voltage of the capacitors C_{f1} and C_{f2} is equal to the sum of the capacitors C_1 and C_2 voltage reflected through the transformer T_2 and the voltage of the capacitor C_2 reflected through the coupled inductor T_1. This topology has two variations: when input inductor is part of T_1, and when it is discrete. In the first case, the input inductor is implemented as the fourth winding of the T_1 with N_{qZ} turns number. Another option is to use a discrete inductor L_1 at the input along with a three-winding coupled inductor in the qZS network. The first topology with a single magnetic component in the IS network is simpler, but has higher input current ripple. The other one with two magnetic components in the qZS network is more complicated, but the input current has lower ripple.

B. Converters With Push–Pull Switching Stage

This group is also based on the combined features of the coupled-inductor topologies with a single switch with those of the transformer-based topologies with a push–pull switching stage (see Fig. 29). Converters within this group operate similarly to those from the previous group.

1) Quasi-Z-Source: Only two topologies based on the qZS network exists in this group (see Fig. 30) [70]. Voltages of the output windings are similar to the previous case. Topological variations are revealed in the implementation of the input inductor. It can be used as a fourth winding of T_1 with a N_{qZ} number of turns, or as a discrete inductor L_1. The input current ripple is higher in the first case, while the second case requires more passive elements.

C. Converters With a Single Switch

Further simplification of the switching stages has led to IS galvanically isolated single-switch dc–dc converters with combined energy transfer. The generalized functional scheme is shown in Fig. 31. It is derived by combining a transformer-based and a coupled-inductor-based single-switch converter. Overall performance of these converters is limited by the power processing capabilities of a single switch.

1) Quasi-Z-Source: The qZS-based converter from this group is an improved transformer-based single-switch topology presented in [64]. The qZS network allows a simple integration of the output windings as shown in Fig. 32. It is achieved due to equal voltages across the input windings of the coupled inductor T_2 and isolation transformer T_1. Here, coupling of the input inductor is also optional. In the simplest case, when a coupled inductor is placed instead of the right qZS inductor, the current ripple of the output windings will be reflected to the qZS network through T_2. It means that the relation between the turns ratios n_1 and n_2 requires additional research to avoid possible discontinuous conduction mode in the input winding of the inductor T_2. The main drawback of this topology is the limited power rating of a single switch, especially when it suffers from high current pulses at the low dc voltage gain. It requires nonzero switch duty cycle to provide voltage at the output.

ISCs topologies with combined energy transfer are brand new and have not been verified experimentally. Furthermore, only qZS-based converters have been proposed in this group. Further research could focus on the application of different ISNs to this concept, as well as on the analysis of the influence of the parasitic components and experimental verification for certain case study systems. It will help to define their overall performance and application range.

VII. Classification and Comparison of IS Galvanically Isolated DC–DC Converters

All the reviewed topologies can be considered as basic topologies. Many other converters could be derived from them by parallel connection of basic topologies without magnetic coupling [71], or with magnetic coupling between ISNs [71], [72]. These basic topologies could be used in different parallel–series energy conversion systems [68], [73]. The implementation of the secondary side with active switches allows bidirectional operation of basic topologies [26], [42].

A. Classification of IS Galvanically Isolated DC–DC Converters

To clarify the derivation process and show the potential gray areas, the existing converters were classified. The reason is that in the classification of ISNs in [2], the essence of the IS dc–dc electric energy conversion remains uncovered and some topologies are neglected. Use of ISNs as the main factor of classification is not a benefit due to their spreading high variety. For example, two novel passive ISNs have been proposed recently: L-Z-source [74] and sigma-Z-source [75]. Also, active ISNs are becoming popular [76], [77]. Moreover, most of the ISNs can be further modified using switched-inductor and switched-capacitor cells [78] or voltage-lift technique [79] to improve the voltage step-up characteristic, or using passive LC- [80], [81] or C-filers [82] to achieve continuous input current. Hence, ISN could not be used as a major factor for classification.

The first level in the classification is based on the energy transfer principle: energy could be transferred from the input to the output side through a transformer, coupled inductor, or based on the combined energy transfer principle. This factor has advantages over the switching stage type since it contains fewer groups, and, thus, results in a better hierarchical structure. Also, the single-switch switching stage is applicable for any type of energy conversion within the IS converters reviewed, while it is impossible to apply each energy conversion type to any type of switching stage.

The second level of classification is based on the implementation of the switching stage. The third level of classification shows the ISNs applied to the basic structures shown in Figs. 8, 13, 16, 20, 22, 24, 27, 29, and 31. The fourth level is used to indicate topological variations of the basic principle defined by the previous three levels. The classification of the state-of-the-art IS galvanically isolated dc–dc converters is shown in Fig. 6. The first two levels define only ten basic principles. Only one or two ISN types were applied to nine of them. This provides further research space for applications of other ISNs.

The converters based on the single-phase qZSI have been studied most extensively. This group has the widest topological variations. The single-phase IS inverter-based group contains more topologies than other groups. The reason is that this derivation principle is natural and the simplest. Numerous IS inverters have been comprehensively investigated. Many of these results could be reused in the dc–dc converter design. The classification proposed shows wide prospects for research of new IS galvanically isolated dc–dc converter topologies on the third and fourth level of the classification. Focus should be on the utilization of ISNs and their topological variations. Furthermore, an extension of the classification at the second level is possible. The application of different switching stages in the class of ISC with combined energy transfer is the most obvious.

Therefore, it is concluded that the proposed classification is versatile, and could be used as a basis for future derivation and systematization of novel IS galvanically isolated dc–dc converters.

B. Control, Application Possibilities, and General Comparison of the IS Galvanically Isolated DC–DC Converters

Table II summarizes all the reviewed basic topologies from the family of IS galvanically isolated dc–dc converters. Thirty topologies are compared according to the number of passive and semiconductor components, and maximum switch duty cycle. In addition, advantages and drawbacks are pointed out. Special attention has been paid to dc voltage gain in the boost mode, since this mode is most common in the reported case study systems. All the expressions are provided for lossless idealized converters. Basic strategies of switching control for the topologies reviewed are shown in Fig. 33 and referenced in Table II to explain the dc voltage gain expressions. In the topologies with symmetrical PWM control, like full-bridge or push–pull, maximum duty cycle of a switch could be related to any switch in the switching stage. Otherwise, it is related to a switch that generates the shoot-through states at the output terminals of an ISN—switch S_2 in the case of the asymmetrical half-bridge IS galvanically isolated dc–dc converters. Maximum duty cycle of a switch depends also on the type of the ISN, especially in the case of the magnetically coupled ISN, where the turns ratio m defines the operation range of the duty cycle referred to the switching period T.

The simple switching control strategies shown in Fig. 33 describe the basic operation of the topologies reviewed. The single-phase full-bridge topologies can be controlled with the symmetrical overlap strategy [see Fig. 33(a)]. It fits also the majority of push–pull converters and symmetrical half-bridge converters since they require only control of two switches S_1 and S_2 with the same sequence. Apparently, the operating frequency of the ISN as well as the frequency of the input current ripple is twice the transistor switching frequency. It could be extended to a three phase as shown in Fig. 33(b), the three-phase bridge operates without zero states, while additional shoot-through states are added at the switching transitions of each leg. It results in sixfold operation frequency of the ISN and high utilization of

TABLE II
COMPARISON OF BASIC TOPOLOGIES OF THE IS GALVANICALLY ISOLATED DC–DC CONVERTERS

TOPOLOGY	MAXIMUM DUTY CYCLE OF A SWITCH	DC VOLTAGE GAIN IN BOOST MODE (CONTROL)	NO. OF SC*		NO. OF MC*			NO. OF C*	PROS (+) AND CONS (-)
			D*	S*	L*	CL*	TR*		
TRANSFORMER BASED									
qZS symmetrical half-bridge converter [58] (Fig. 14)	0.75	$\frac{n}{(1-2\cdot D_S)}$ (Fig. 33*a*)	4	2	4	0	1	6	+ double input possibility + low number of switches + continuous input current - high number of passive components - high voltage stress of switches
qZS asymmetrical half-bridge converter with 1 capacitors [59] (Fig. 15*b*)	0.5 (S_2 on Fig. 15)	$\frac{n}{(1-2\cdot D)}$ (Fig. 33*c*)	3	2	2	0	1	6	+ low number of components + continuous input current - DC blocking capacitor is needed - uneven loading of switches - high voltage stress of switches
qZS asymmetrical half-bridge converter with 2 capacitors [59] (Fig. 15*a*)			3	2	2	0	1	7	
qZS single-switch converter [64] (Fig. 21)	0.5	$\frac{n}{(1-2\cdot D)}$ (Fig. 33*e*)	3	1	2	0	1	5	+ low number of components + continuous input current - DC blocking capacitor is needed - high stress of a switch
ZS three-phase full-bridge converter [21] (Fig. 5*b*)	0.75	$\frac{2\cdot n}{(1-2\cdot D_S)}$ (Fig. 33*b*)	7	6	3	0	1	3	+ better power density - limited performance due to LC filter - discontinuous input current - high number of SCs
qZS three-phase full-bridge converter [44] (Fig. 10*c*)			5	6	2	0	1	4	+ better power density + continuous input current - high number of SCs
TZS single-phase full-bridge converter [57] (Fig. 12*a*)	$0.5+\frac{1}{2\cdot(1+m)}$	$\frac{2\cdot n}{(1-(1+m)\cdot D_S)}$ (Fig. 33*a*)	3	4	0	1	1	3	+ high voltage step-up at the input stage + low number of passive components - high voltage stress of switches - discontinuous input current
TqZS single-phase full-bridge converter [57] (Fig. 12*b*)			3	4	0	1	1	3	
ZS single-phase full-bridge converter with separated inductors [13] (Fig. 5*a*)	0.75	$\frac{n\cdot(1-D_S)}{(1-2\cdot D_S)}$ (Fig. 33*a*)	5	4	3	0	1	3	- discontinuous input current - limited performance due to LC filter
ZS single-phase series resonant full-bridge converter [24] (Fig. 9)	0.75	$\frac{n}{(1-2\cdot D_S)}$ (Fig. 33*a*)	5	4	3	0	1	4	+ resonant soft switching + high power density - complicated control - discontinuous input current
qZS single-phase full-bridge converter with separated inductors [44] (Fig. 10*a*)	0.75	$\frac{2\cdot n}{(1-2\cdot D_S)}$ (Fig. 33*a*)	3	4	2	0	1	4	+ continuous input current - relatively high number of PCs*
qZS single-phase full-bridge converter with coupled inductor [45] (Fig. 10*b*)	0.75		3	4	0	1	1	4	+ continuous input current + magnetically integrated ISN - relatively high number of PCs*
qZS single-phase series resonant full-bridge converter [48] (Fig. 10*d*)	0.75		3	4	3	0	1	5	+ continuous input current + resonant soft switching - variable frequency control
qZS single-phase full-bridge converter with synchronous rectification [27] (Fig. 10*e*)	0.75 (S_1…S_4) 1.0 (S_D) 0.5 (S_{r1}…S_{r2})		0	7	2	0	1	4	+ low losses and high power density + continuous input current - high number of SCs - lower reliability
Cascaded CAEB qZS single-phase full-bridge converter [17] (Fig. 11)	2/3	$\frac{2\cdot n}{(1-3\cdot D_S)}$ (Fig. 33*a*)	4	4	3	0	1	6	+ continuous input current + high voltage step-up at the input stage - high number of passive components
YS push-pull converter [62] (Fig. 19)	$\frac{(1+m)}{2\cdot m}$	$\frac{2\cdot n}{(1-m\cdot D_S)}$ (Fig. 33*a*)	3	2	0	1	1	3	+ high voltage step-up at the input stage + low number of components + magnetically integrated ISN - complicated design of ISN - discontinuous input current - high voltage stress of switches - three-winding transformer

TOPOLOGY	MAXIMUM DUTY CYCLE OF A SWITCH	DC VOLTAGE GAIN IN BOOST MODE (CONTROL)	NO. OF SC*		NO. OF MC*			NO. OF C*	PROS (+) AND CONS (-)
			D*	S*	L*	CL*	TR*		
qZS push-pull converter with separated inductors [61] (Fig. 18)	0.75	$\frac{2\cdot n}{(1-2\cdot D_S)}$ (Fig. 33a)	3	2	2	0	1	4	+ low number of SCs + continuous input current - high voltage stress of switches - three-winding transformer
qZS push-pull converter with coupled inductor [60] (Fig. 17*a*)	0.75		3	2	0	1	1	4	+ low number of SCs + continuous input current + magnetically integrated ISN - high voltage stress of switches - three-winding transformer
Coupled qZS interleaved push-pull converter [60] (Fig. 17*b*)	0.5	$\frac{2\cdot n}{(1-2\cdot D)}$ (Fig. 33*d*)	4	2	0	1	1	6	+ low number of SCs + continuous input current - complicated design of ISN - high voltage stress of switches - high number of passive components
COUPLED INDUCTOR BASED									
ZS single-switch converter [69] (Fig. 26)	0.5	$\frac{2\cdot n\cdot(1+D)}{(1-2\cdot D)}$ (Fig. 33*e*)	4	1	0	2	0	6	+ single switch - discontinuous input current - high number of semiconductor components
qZS single-switch converter with a single inductor [68] (Fig. 25*b*)	0.5	$\frac{n}{(1-2\cdot D)}$ (Fig. 33*e*)	3	1	0	1	0	4	+ single switch + high magnetic integration + continuous input current
qZS single-switch converter with two inductors [67] (Fig. 25*a*)	0.5	$\frac{2\cdot n\cdot(1+D)}{(1-2\cdot D)}$ (Fig. 33*e*)	4	1	1	1	0	6	+ single switch + continuous input current - high number of components
qZS push-pull converter with a single inductor [66] (Fig. 23*b*)	0.5	$\frac{2\cdot n\cdot D}{(1-2\cdot D)}$ (Fig. 33*d*)	6	2	1	1	0	5	+ continuous input current + high magnetic integration of ISN - limited performance due to LC filter - high number of components
qZS push-pull converter with two inductors [65] (Fig. 23*a*)	0.5		6	2	1	2	0	5	+ continuous input current - limited performance due to LC filter - high number of components
WITH COMBINED ENERGY TRANSFER									
qZS single-phase full-bridge converter with a single inductor [70] (Fig. 28)	0.75	$2\cdot\frac{n_1\cdot D_S+n_2}{(1-2\cdot D_S)}$ (Fig. 33*a*)	3	4	0	1	1	4	+ high magnetic integration of ISN + additional voltage step-up + continuous input current - complicated design of CL - high input current ripple
qZS single-phase full-bridge converter with two inductors [70] (Fig. 28)			3	4	1	1	1	4	+ additional voltage step-up + continuous input current - complicated design of CL
qZS push-pull converter with a single inductor [70] (Fig. 30)			3	2	0	1	1	4	+ high magnetic integration of ISN + additional voltage step-up + continuous input current - complicated design of CL - high input current ripple
qZS push-pull converter with two inductors [70] (Fig. 30)			3	2	1	1	1	4	+ additional voltage step-up + continuous input current - complicated design of CL
qZS single-switch converter with a single inductor [64] (Fig. 32)	0.5	$\frac{(n_1+n_2)}{(1-2\cdot D_S)}$ (Fig. 33*e*)	3	1	0	1	1	5	+ high magnetic integration of ISN + additional voltage step-up + continuous input current - high stress of a switch - high input current ripple
qZS single-switch converter with two inductors [64] (Fig. 32)	0.5		3	1	1	1	1	5	+ additional voltage step-up + continuous input current - high stress of a switch

*SC – semiconductor component; MC – magnetic component; D – diode; S – switch; L – inductor; CL – coupled inductor; TR – transformer; C – capacitor; PC – passive component.

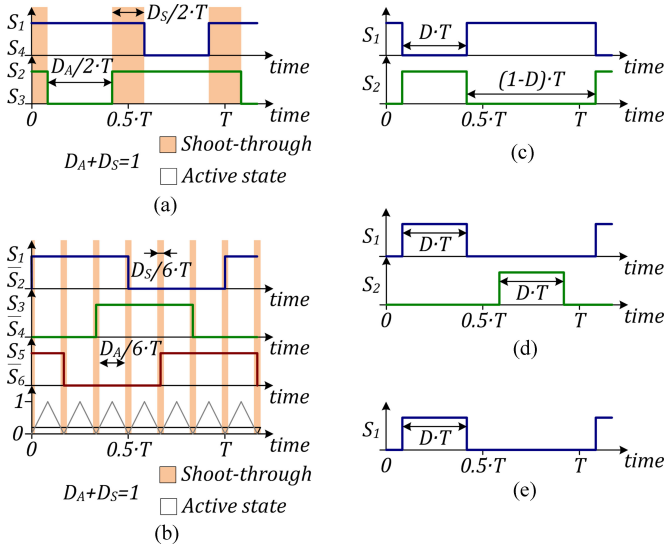

Fig. 33. Simplified switching control strategies for: (a) single-phase full-bridge, symmetrical half-bridge, and majority of push–pull topologies, (b) three-phase full-bridge topologies, (c) asymmetrical half-bridge topologies, (d) interleaved push–pull topologies, and (e) single-switch topologies.

the isolation transformer in high-power applications. Overlap of switches control signals is not required in interleaved topologies, transformer-based interleaved push–pull and coupled-inductor-based push–pull, since switches perform short-circuiting of the ISN output terminals directly. In this case, interleaved control [see Fig. 33(d)] with 180° phase shift results in lower input current ripple and ISN operating frequency doubling. Asymmetrical half-bridge topologies require asymmetrical control [see Fig. 33(c)], while single-switch topologies utilize simple control [see Fig. 33(e)] where the duty cycle of the switch is limited (see Table II). These topologies with reduced number of switches have reduced operating frequency of the ISN, which is equal to the transistor(s) switching frequency.

The converters reviewed reveal their advantages in applications where a wide input voltage regulation range is required. Recent areas mostly include renewable and alternative energy applications. Usually it means low-voltage input and handling relatively high current. Most of the ISNs have a diode that results in relatively high losses at the input side. Maximum reported peak efficiency is in the range of 96%–97% [24], [61], [62]. It is mostly measured without voltage step-up at the input side, i.e. at maximum rated input voltage. Regulation range is usually limited with an efficiency drop and is often within the range 1:3 for simpler ISNs and a slightly wider range for those magnetically coupled. At maximum voltage step-up, i.e., minimum rated input voltage, the efficiency could drop to 85%, depending on the application and the hardware used. This trend is the same for transformer-based and coupled-inductor-based converters, and, thus, the efficiency of converters with combined energy transfer is in the same range too. Recently several approaches, like series resonance and synchronous rectification, have been proposed to reduce power loss. Synchronous rectification in the ISN is most advantageous among the results reported. Further efficiency improvement could be achieved with soft switching in power switches. Efficiency optimization is a crucial issue for power electronics systems and further studies of IS converters are required. Apparently, there is still a room for improvement in the new field of IS dc–dc converter technology.

Application possibilities for IS dc–dc converters need further examination, since reports on case study systems are scarce. In most of the examples available, emerging applications of the single-phase full-bridge qZS converter are numerous. However, it is not an appropriate conclusion that ISCs can be used only with low-voltage input. Application examples that contain experimental verification are described below for all the applications reported.

The area of *wind energy* has benefited from two different types of IS converters. It is one of the most demanding renewable energy applications due to a wide range of output voltage variations of the wind turbine, especially for those based on PMSG. The transformer-based qZS full-bridge dc–dc converter has been used together with an active rectifier in the interface converter for residential PMSG-based wind turbines with a rated power of 1.3 kW [47]. The total voltage gain of the interface converter was distributed between the input side active rectifier and the qZS converter. The active rectifier was used to stabilize the first dc-link voltage at low wind speeds at the level of 150 V, while uncontrolled rectification was performed at higher wind speeds when the generator is able to provide dc-link voltage higher than 150 V. The qZS converter was used to stabilize the second dc-link voltage, which feeds the grid-side inverter at the level of 250 V. It means that the transformer-based qZS full-bridge converter was operating at a voltage boost lower than twofold, which is within the recommended range of 1:3. Application of the coupled-inductor-based qZS push–pull converter together with the uncontrolled six-pulse three-phase diode rectifier to exactly the same wind turbine was described in [83]. The qZS converter there covers the whole operating voltage range of the wind turbine from 65 to 259 V in the boost mode only. Hence, the coupled-inductor qZS push–pull converter has shown an ability to operate in the range of 1:4. Its operation in the range from 40 to 400 V is described in [3], where efficiency higher than 90% was achieved for the 1:4 input voltage range from 100 to 400 V at the maximum input current. High efficiency at the switching frequency of 100 kHz was assured by the SiC devices, which are essential to realize the high-frequency high-voltage IS converters [40]. The coupled-inductor topology has used nearly the same inductance in the qZS network (1 mH) as the transformer-based counterpart, while the input current ripple was higher due to the different operating principle, but this is not a weighty disadvantage since the dc-link capacitor on the generator side decouples current ripple from the generator. However, the design and operation principle of the coupled-inductor-based qZS topology is more complicated, and, thus, more efforts may be required to build such systems.

Photovoltaic power generation systems are also an attractive area of application for the IS dc–dc converters. For example, a microconverter realized with the transformer-based qZS symmetrical half-bridge topology was proposed in [58] for integration of single or two PV panels into the common dc bus. The concept was verified for operation at constant input current 5 A

and input voltage range from 30 to 58 V, i.e., the rated power is 300 W. Such operating conditions with constant input current are common for PV maximum power point trackers when the input voltage of the converter changes with the PV panel temperature, while the input current remains nearly constant at the same irradiation. The obtained efficiency was around 92% at the switching frequency 100 kHz, since no optimization of losses was involved.

Fuel cells are more demanding than photovoltaic and wind turbine applications. They provide maximum output power at the minimum output voltage, while renewable applications usually provide maximum output power at the maximum output voltage. An industrial converter based on the galvanically isolated qZS full-bridge dc–dc converter is proposed for proton exchange membrane fuel cells with power up to 8 kW in [84]. It was created in cooperation between the Tallinn University of Technology and industrial partners. The grid-connected interface performs energy conversion in two stages. The first stage contains two qZS full-bridge converters that operate in parallel with interleaved control and stabilize dc-link voltage at the level of 600 V. Stable voltage is used to supply the grid-side three-phase inverter at the second stage. The input voltage range is from 35 to 64 V, while the input current can reach up to 230 A. The peak efficiency achieved was around 96%.

Power factor corrector (PFC) based on the galvanically isolated qZS full-bridge topology with rated power of 1 kW was proposed in [85]. It supplies load with 380 V dc voltage from 230 V/60 Hz grid voltage, which is rectified by a single-phase bridge diode rectifier. The PFC was designed to operate with 20% input current ripple at the switching frequency of 50 kHz, which results in the 1 mH value of qZS network inductors. This allowed 4.4% of grid current THD to be achieved at full power with an efficiency of 93%.

All the examples for application described above prove high versatility of the IS dc–dc electric energy conversion technology. It can handle different levels of power and input voltage. However, not all of the topologies reviewed in this paper were verified experimentally. Only a few of them were used in practical applications reviewed above. It means that more application oriented research is required to find out applications advantageous for each class of the converters reviewed and define their limitations. As for now, the qZS full-bridge topology was applied to most of the emerging applications and can be selected by engineers to minimize risks regarding the implementation of new topologies in the industrial products.

The main tendency for topology selection at the required power level is the same as for conventional VSCs and CSCs; more complicated topologies with higher number of switches, like full-bridge, fit better for high power applications. For example, push–pull topologies could be used up to medium power levels or for high-current applications, where the number of switches increases the conduction losses. Low power applications benefit from simple topologies, like that with a single switch. Among the three proposed classes of converters, the transformer-based converters cover the whole power range, while they have a simple design procedure. As for now, the coupled-inductor-based converters have been tested only for low power applications (up to 1.5 kW), and, thus, cannot be recommended for higher power levels. The converters with combined energy transfer have not been reported for any applications. They seem to be useful for different power ranges due to the possibility to utilize various switching stage types, but this is not proven yet. Also, they could be applied where a wide input voltage regulation range is necessary if experimental verification proves theoretical predictions. According to design complexity, the transformer-based converters are the simplest, while the coupled inductor based could take more efforts. In terms of design, the converters with combined energy transfer could be most complicated, since it is required to design both an isolation transformer and a coupled inductor and select the right proportion between their turns ratios, while better dc voltage gain could be achieved.

The application of magnetically coupled ISNs, like qTZS or Γ-source, in dc–dc converters needs a separate coverage. They have high performance in inverter use due to high dc voltage gain that leads to smaller loss of the modulation factor control range. This feature is not essential for dc–dc converters in most of the cases, since the main voltage step-up is usually obtained with a transformer and an output rectifier. The ISN is mostly used to adjust the transformer voltage when the input voltage varies. However, the magnetically coupled ISNs could be advantageous in specific applications. For example, the YS push–pull converter could be beneficial in applications with very low input voltage and relatively high input current. In this case, the transformer design could be complicated if a simpler ISN is used. The input voltage could be preadjusted with the YS network up to an acceptable level, while the push–pull switching stage provides low conduction losses with high input current.

In Table II, the converters reviewed are compared on the basis of the qZS full-bridge topology with separated inductors mostly due to their continuous input current, which is highly demanded for emerging applications. They have no obvious disadvantages revealed from the comparison with other converters. Their disadvantages, like relatively low efficiency and higher number of components as compared to VSCs and CSCs, are common for all converters from this review and balanced with improved regulation range and reliability. Data in Table II prove that the basic topology selected could be a preferable solution for emerging applications.

VIII. Conclusion

The modern renewable energy market requires versatile power electronics solutions. The review in this paper reveals that the qZS-based galvanically isolated dc–dc converters can be further developed as the basic power electronics building blocks for dispersed generation systems.

The proposed classification of the isolated IS dc–dc converters shows numerous gaps in this field mostly related to the application of certain ISN to the generalized topology structure or application of another switching stage to a certain energy transfer principle. It could be concluded that converters from the transformer-based class are simpler to design, more

flexible, and have a wider application range. Coupled-inductor-based topologies are more complicated to design and control and less effective, but they show better performance where a wide voltage regulation range is needed. They are required only in some applications with wide input voltage variations, for instance, in PMSG-based wind turbines. The converters with combined energy transfer proposed recently require extensive research.

Numerous further research areas are indicated in this paper. Ten generalized functional schemes proposed can be used to understand the derivation process of the IS galvanically isolated dc–dc converter topologies or as a derivation tool.

Finally, it is concluded that broadly, the qZS-based converters have advantages over other IS topologies for emerging applications. Further directions to improve those converters were discussed. Main directions for future research are the resonant implementations, active rectification in the input and the output sides, bidirectional operation, and also the use of new materials and semiconductors, which might give a new paradigm of converter design.

REFERENCES

[1] F. Z. Peng, "Z-source inverter," *IEEE Trans. Ind. Appl.*, vol. 39, no. 2, pp. 504–510, Mar./Apr. 2003.

[2] Y. P. Siwakoti, F. Z. Peng, F. Blaabjerg, P. C. Loh, and G. E. Town, "Impedance source networks for electric power conversion part I: a topological review," *IEEE Trans. Power Electron.*, vol. 30, no. 2, pp. 699–716, Feb. 2015.

[3] A. Chub, O. Husev, and D. Vinnikov, "Comparative study of rectifier topologies for quasi-Z-source derived push-pull converter," *Electron. Electr. Eng.*, vol. 20, no. 6, pp. 29–34, Jun. 2014.

[4] A. Andrijanovits, A. Blinov, D. Vinnikov, and J. Martins. (2012). Magnetically coupled multiport converter with integrated energy storage. *Electr. Rev.* [Online]. 88(7b), pp. 171–176. Available: http://pe.org.pl/articles/2012/7b/44.pdf

[5] J. Zakis, D. Vinnikov, O. Husev, and I. Rankis, "Dynamic behaviour of qZS-based bi-directional DC-DC converter in supercapacitor charging mode," in *Proc. Int. Symp. Power Electron. Electr. Drives, Autom. Motion*, Jun. 20–22, 2012, pp. 764–768.

[6] B. Zhao, Q. Yu, Z. Leng, and X. Chen, "Switched Z-source isolated bidirectional DC–DC converter and its phase-shifting shoot-through bivariate coordinated control strategy," *IEEE Trans. Ind. Electron.*, vol. 59, no. 12, pp. 4657–4670, Dec. 2012.

[7] X. Li, M. Zhu, J. Zhang, and X. Cai, "Modeling and close-loop control strategies of switched Z-source isolated bidirectional DC-DC converter," in *Proc. Int. Electron. Appl. Conf. Expo.*, Nov. 5–8, 2014, pp. 997–1002.

[8] Y. Liu, H. Abu-Rub, and B. Ge, "Z-source/quasi-Z-source inverters: Derived networks, modulations, controls, and emerging applications to photovoltaic conversion," *IEEE Ind. Electron. Mag.*, vol. 8, no. 4, pp. 32–44, Dec. 2014.

[9] Z. Rasin, K. Ahsanullah, and M. F. Rahman, "Design and simulation of quasi-Z-source grid-connected PV inverter with bidirectional power flow for battery storage management," in *Proc. IEEE 39th Annu. Conf. Ind. Electron. Soc.*, Nov. 10–13, 2013, pp. 1589–1594.

[10] I. Roasto, D. Vinnikov, J. Zakis, and O. Husev, "New shoot-through control methods for qZSI-based DC-DC converters," *IEEE Trans. Ind. Informat.*, vol. 9, no. 2, pp. 640–647, May 2013.

[11] M. Kasper, M. Ritz, D. Bortis, and J. W. Kolar, "PV panel-integrated high step-up high efficiency isolated GaN DC-DC boost converter," in *Proc. 35th Int. Telecommun. Energy Conf.*, Oct. 13–17, 2013, pp. 1–7.

[12] T. LaBella and J. S. Lai, "A hybrid resonant converter utilizing a bidirectional GaN AC switch for high-efficiency PV applications," in *Proc. IEEE 29th Annu. Appl. Power Electron. Conf. Expo.*, Mar. 16–20, 2014, pp. 1–8.

[13] D. Vinnikov, I. Roasto, and T. Jalakas, "New step-up DC-DC converter with high-frequency isolation," in *Proc. IEEE 35th Annu. Conf. Ind. Electron. Soc.*, Nov. 3–5, 2009, pp. 670–675.

[14] V. P. Galigekere and M. K. Kazimierczuk, "Analysis of PWM Z-source DC-DC converter in CCM for steady state," *IEEE Trans. Circuits Syst. I, Reg. Papers*, vol. 59, no. 4, pp. 854–863, Apr. 2012.

[15] J. Anderson and F. Z. Peng, "Four quasi-Z-source inverters," in *Proc. IEEE Power Electron. Spec. Conf.*, Jun. 15–19, 2008, pp. 2743–2749.

[16] V. Vaisanen, T. Riipinen, J. Hiltunen, and P. Silventoinen, "Design of 10 kW resonant push-pull DC-DC converter for solid oxide fuel cell applications," in *Proc. 14th Eur. Conf. Power Electron. Appl.*, Aug. 30/Sept. 1, 2011, pp. 1–10.

[17] D. Vinnikov, I. Roasto, R. Strzelecki, and M. Adamowicz, "Step-up DC-DC converters with cascaded quasi-Z-source network," *IEEE Trans. Ind. Electron.*, vol. 59, no. 10, pp. 3727–3736, Oct. 2012.

[18] M. Mohr and F. W. Fuchs, "Clamping for current-fed dc/dc converters with recovery of clamping energy in fuel cell inverter systems," in *Proc. Eur. Conf. Power Electron. Appl.*, Sep. 2–5, 2007, pp. 1–10.

[19] J. Zakis, D. Vinnikov, V. Kolosov, and E. Vasechko, "New active clamp circuit for current-fed galvanically isolated DC-DC converters," in *Proc. 8th Int. Conf. Workshop Compat. Power Electron.*, Jun. 5–7, 2013, pp. 353–358.

[20] L. Zhu, K. Wang, F. C. Lee, and J.-S. Lai, "New start-up schemes for isolated full-bridge boost converters," *IEEE Trans. Power Electron.*, vol. 18, no. 4, pp. 946–951, Jul. 2003.

[21] M. Egorov, D. Vinnikov, R. Strzelecki, and M. Adamowicz, "Impedance source inverter based high-power DC-DC converter for fuel cell applications," in *Proc. 8th Int. Conf. Environ. Electr. Eng.*, May 10–13, 2009, pp. 1–4.

[22] D. Vinnikov, I. Roasto, and T. Jalakas, "An improved high-power DC-DC converter for distributed power generation," in *Proc. 10th Int. Conf. Electr. Power Qual. Utilisation*, Sep. 15–17, 2009, pp. 1–6.

[23] I. Roasto, D. Vinnikov, T. Jalakas, J. Zakis, and S. Ott, "Experimental study of shoot-through control methods for qZSI-based DC-DC converters," in *Proc. Int. Symp. Power Electron. Electr. Drives, Autom. Motion*, Jun. 14–16, 2010, pp. 29–34.

[24] H. Cha, F. Z. Peng, and D. Yoo, "Z-source resonant DC-DC converter for wide input voltage and load variation," in *Proc. 9th Int. Power Energy Conf.*, Jun. 21–24, 2010, pp. 995–1000.

[25] L. Liivik, D. Vinnikov, and T. Jalakas "Synchronous rectification in quasi-Z-source converters: possibilities and challenges," in *Proc. IEEE Int. Conf. Intell. Energy Power Syst.*, Jun. 2–6, 2014, pp. 32–35.

[26] J. Zakis, D. Vinnikov, I. Roasto, and L. Ribickis, "Quasi-Z-source inverter based bi-directional DC-DC converter: Analysis of experimental results," in *Proc. 7th Int. Conf. Workshop Compat. Power Electron.*, Jun. 1–3, 2011, pp. 394–399.

[27] L. Liivik, D. Vinnikov, and J. Zakis, "Simulation study of high step-up quasi-Z-source DC-DC converter with synchronous rectification," in *Proc. 55th Int. Sci. Conf. Power Electr. Eng. Riga Tech. Univ.*, Oct. 14, 2014, pp. 34–37.

[28] M. Acanski, J. Popovic-Gerber, and J. A. Ferreira, "Comparison of Si and GaN power devices used in PV module integrated converters," in *Proc. IEEE Energy Convers. Congr. Expo.*, Sep. 17–22, 2011, pp. 1217–1223.

[29] Y. Zhou, L. Liu, and H. Li, "A high-performance photovoltaic module-integrated converter (MIC) based on cascaded quasi-Z-source inverters (qZSI) using eGaN FETs," *IEEE Trans. Power Electron.*, vol. 28, no. 6, pp. 2727–2738, Jun. 2013.

[30] D. Han and B. Sarlioglu, "Dead-time effect on GaN-based synchronous boost converter and analytical model for optimal dead-time selection," *IEEE Trans. Power Electron.*, 2015, to be published.

[31] L. Garcia-Rodriguez, E. Williams, J. C. Balda, J. Gonzalez-Llorente, E. Lindstrom, and A. Oliva, "Dual-stage microinverter design with a GaN-based interleaved flyback converter stage," in *Proc. IEEE Energy Convers. Congr. Expo.*, Sep. 15–19, 2013, pp. 4496–4502.

[32] D. Reusch and J. Strydom, "Evaluation of gallium nitride transistors in high frequency resonant and soft-switching DC-DC converters," *IEEE Trans. Power Electron.*, vol. 30, no. 9, pp. 5151–5158, Sep. 2015.

[33] A. Lidow, J. Strydom, M. De Rooij, and D. Reusch, *GaN Transistors for Efficient Power Conversion*, 2nd ed. New York, NY, USA: Wiley, 2014.

[34] X. Ren, D. Reusch, S. Ji, Z. Zhang, M. Mu, and F. C. Lee, "Three-level driving method for GaN power transistor in synchronous buck converter," in *Proc. IEEE Energy Convers. Congr. Expo.*, Sep. 15–20, 2012, pp. 2949–2953.

[35] D. Reusch and J. Strydom, "Understanding the effect of PCB layout on circuit performance in a high-frequency gallium-nitride-based point of load converter," *IEEE Trans. Power Electron.*, vol. 29, no. 4, pp. 2008–2015, Apr. 2014.

[36] A. Kadavelugu, S. Baek, S. Dutta, S. Bhattacharya, M. Das, A. Agarwal, and J. Scofield, "High-frequency design considerations of dual active bridge 1200 V SiC MOSFET DC-DC converter," in *Proc. IEEE 26th Annu. Appl. Power Electron. Conf. Expo.*, Mar. 6–11, 2011, pp. 314–320.

[37] A. Kadavelugu, V. Baliga, S. Bhattacharya, M. Das, and A. Agarwal, "Zero voltage switching performance of 1200 V SiC MOSFET, 1200V silicon IGBT and 900V CoolMOS MOSFET," in *Proc. IEEE Energy Convers. Congr. Expo.*, Sep. 17–22, 2011, pp. 1819–1826.

[38] J. A. Carr, D. Hotz, J. C. Balda, H. A. Mantooth, A. Ong, and A. Agarwal, "Assessing the impact of SiC MOSFETs on converter interfaces for distributed energy resources," *IEEE Trans. Power Electron.*, vol. 24, no. 1, pp. 260–270, Jan. 2009.

[39] J. Biela, M. Schweizer, S. Waffler, and J. W. Kolar, "SiC versus Si—Evaluation of potentials for performance improvement of inverter and DC-DC converter systems by SiC power semiconductors," *IEEE Trans. Ind. Electron.*, vol. 58, no. 7, pp. 2872–2882, Jul. 2011.

[40] A. Blinov, A. Chub, D. Vinnikov, and T. Rang, "Feasibility study of Si and SiC MOSFETs in high-gain DC-DC converter for renewable energy applications," in *Proc. IEEE 39th Annu. Conf. Ind. Electron. Soc.*, Nov. 10–13, 2013, pp. 5975–5978.

[41] A. F. Witulski, "Introduction to modeling of transformers and coupled inductors," *IEEE Trans. Power Electron.*, vol. 10, no. 3, pp. 349–357, May 1995.

[42] B. Zhao, Q. Yu, Z. Leng, and X. Chen, "Switched Z-source isolated bidirectional DC-DC converter and its phase-shifting shoot-through bivariate coordinated control strategy," *IEEE Trans. Ind. Electron.*, vol. 59, no. 12, pp. 4657–4670, Dec. 2012.

[43] H. Cha, F. Z. Peng, and D. Yoo, "Distributed impedance network (Z-network) DC-DC converter," *IEEE Trans. Power Electron.*, vol. 25, no. 11, pp. 2722–2733, Nov. 2010.

[44] D. Vinnikov and I. Roasto, "Quasi-Z-source-based isolated DC-DC converters for distributed power generation," *IEEE Trans. Ind. Electron.*, vol. 58, no. 1, pp. 192–201, Jan. 2011.

[45] J. Zakis, D. Vinnikov, and L. Bisenieks, "Some design considerations for coupled inductors for integrated buck-boost converters," in *Proc. IEEE Int. Conf. Power Eng., Energy Electr. Drives, POWERENG*, May 11–13, 2011, pp. 1–6.

[46] D. Vinnikov, I. Roasto, J. Zakis, and R. Strzelecki. (2010). New step-up DC-DC converter for fuel cell powered distributed generation systems: Some design guidelines. *Electr. Rev.* [Online]. 86(8), pp. 245–252. Available: http://pe.org.pl/abstract_pl.php?nid = 4109

[47] D. Vinnikov, L. Bisenieks, and I. Galkin. (2012). New isolated interface converter for PMSG based variable speed wind turbines. *Electr. Rev.* [Online]. 88(1a), pp. 75–80. Available: http://pe.org.pl/articles/2012/1a/15.pdf

[48] J. Zakis, I. Rankis, and L. Liivik, "Loss reduction method for the isolated qZS-based DC-DC converter," *Electr. Control Commun. Eng.*, vol. 4, pp. 13–18, 2013..

[49] J. Zakis, I. Rankis, and L. Ribickis, "Comparative analysis of boost and quasi-Z-source converters as maximum power point trackers for PV panel integrated converters," in *Proc. IEEE 23rd Int. Symp. Ind. Electron.*, Jun. 1–4, 2014, pp. 1991–1995.

[50] P. Xuewei and A. K. Rathore, "Current-fed soft-switching push–pull front-end converter-based bidirectional inverter for residential photovoltaic power system," *IEEE Trans. Power Electron.*, vol. 29, no. 11, pp. 6041–6051, Nov. 2014.

[51] P. Xuewei, A. K. Rathore, and U. R. Prasanna, "Novel soft-switching snubberless naturally clamped current-fed full-bridge front-end-converter-based bidirectional inverter for renewables, microgrid, and UPS applications," *IEEE Trans. Ind. Appl.*, vol. 50, no. 6, pp. 4132–4141, Nov./Dec. 2014.

[52] D. R. Nayanasiri, G. H. B. Foo, D. M. Vilathgamuwa, and D. L. Maskell, "A switching control strategy for single- and dual-inductor current-fed push–pull converters," *IEEE Trans. Power Electron.*, vol. 30, no. 7, pp. 3761–3771, Jul. 2015.

[53] D. Vinnikov, I. Roasto, T. Jalakas, R. Strzelecki, and M. Adamowicz. (2012). Analytical comparison between capacitor assisted and diode assisted cascaded quasi-Z-source inverters. *Electr. Rev.* [Online]. 88(1a), pp. 212–217. Available: http://pe.org.pl/articles/2012/1a/45.pdf

[54] P. C. Loh, D. Li, and F. Blaabjerg, "Γ-Z-source inverters," *IEEE Trans. Power Electron.*, vol. 28, no. 11, pp. 4880–4884, Nov. 2013.

[55] W. Qian, F. Z. Peng, and H. Cha, "Trans-Z-source inverters," *IEEE Trans. Power Electron.*, vol. 26, no. 12, pp. 3453–3463, Dec. 2011.

[56] Y. P. Siwakoti, P. C. Loh, F. Blaabjerg, and G. E. Town, "Y-source impedance network," *IEEE Trans. Power Electron.*, vol. 29, no. 7, pp. 3250–3254, Jul. 2014.

[57] M.-K. Nguyen, Q.-D. Phan, V.-N. Nguyen, Y.-C. Lim, and J.-K. Park, "Trans-Z-source-based isolated DC-DC converters," in *Proc. IEEE 22nd Int. Symp. Ind. Electron.*, May 28–31, 2013, pp. 1–6.

[58] D. Vinnikov, A. Chub, O. Husev, and T. Jalakas, "Quasi-Z-source half-bridge DC-DC converter for photovoltaic applications," in *Proc. IEEE Int. Conf. Ind. Technol.*, Mar. 17–19, 2015, pp. 2935–2940.

[59] D. Vinnikov, A. Chub, and L. Liivik "Asymmetrical quasi-Z-source half-bridge DC-DC converters," in *Proc. 9th Int. Conf. Compat. Power Electron.*, Jun. 24–26, 2015, pp. 369–372.

[60] A. Chub, O. Husev, D. Vinnikov, and F. Blaabjerg, "Novel family of quasi-Z-source DC-DC converters derived from current-fed push-pull converters," in *Proc. 16th Conf. Power Electron. Appl.*, Aug. 26–28, 2014, pp. 1–10.

[61] Y. P. Siwakoti, F. Blaabjerg, P. C. Loh, and G. E. Town, "High-voltage boost quasi-Z-source isolated DC/DC converter," *IET Power Electron.*, vol. 7, no. 9, pp. 2387–2395, Sep. 2014.

[62] Y. P. Siwakoti, P. C. Loh, F. Blaabjerg, and G. E. Town, "Magnetically coupled high-gain Y-source isolated DC/DC converter," *IET Power Electron.*, vol. 7, no. 11, pp. 2817–2824, Nov. 2014.

[63] Y. P. Siwakoti, P. C. Loh, F. Blaabjerg, and G. E. Town, "Effects of leakage inductances on magnetically coupled Y-source network," *IEEE Trans. Power Electron.*, vol. 29, no. 11, pp. 5662–5666, Nov. 2014.

[64] A. Chub and D. Vinnikov, "Single-switch galvanically isolated quasi-Z-source DC-DC converter," in *Proc. 5th Int. Conf. Power Eng., Energy Elect. Drives, POWERENG*, May 11–13, 2015, pp. 1–5.

[65] D. Vinnikov, J. Zakis, O. Husev, and R. Strzelecki, "New high-gain step-up DC-DC converter with high-frequency isolation," in *Proc. IEEE 27th Annu. Appl. Power Electron. Conf. Expo.*, Feb. 5–9, 2012, pp. 1204–1209.

[66] A. Chub, O. Husev, A. Blinov, and D. Vinnikov. (2014, Sep.). CCM and DCM analysis of quasi-Z-source derived push-pull DC-DC converter. *Informacije MIDEM, J. Microelectron. Electron. Compon. Mater.* [Online]. 44(3), pp. 224–234. Available: http://ojs.midem-drustvo.si/index.php/InfMIDEM/article/view/82/57

[67] F. Evran and M. T. Aydemir, "Z-source-based isolated high step-up converter," *IET Power Electron.*, vol. 6, no. 1, pp. 117–124, Jan. 2013.

[68] A. Chub, O. Husev, and D. Vinnikov, "Input-parallel output-series connection of isolated quasi-Z-source DC-DC converters," in *Proc. Electr. Power Qual. Supply Rel. Conf.*, Jun. 11–13, 2014, pp. 1–8.

[69] F. Evran, and M. T. Aydemir, "Isolated high step-up DC-DC converter with low voltage stress," *IEEE Trans. Power Electron.*, vol. 29, no. 7, pp. 3591–3603, Jul. 2014.

[70] A. Chub and D. Vinnikov, "Quasi-Z-source isolated DC-DC converters with combined energy transfer for renewable energy sources integration," in *Proc. IEEE Int. Conf. Ind. Technol.*, Mar. 17–19, 2015, pp. 2896–2900.

[71] H. Lee, H. Cha, H.-G. Kim, and D. Yoo, "Parallel operation of qZ-source full-bridge DC-DC converter using coupled inductors," in *Proc. IEEE Veh. Power Propul. Conf.*, Oct. 9–12, 2012, pp. 659–666.

[72] H. Lee, H.-G. Kim, and H. Cha, "Parallel operation of trans-Z-source network full-bridge dc-dc converter for wide input voltage range," in *Proc. 7th Int. Power Electron. Motion Control Conf.*, Jun. 2–5, 2012, vol. 3, pp. 1707–1712.

[73] C. Martinez, T. Jalakas, D. Vinnikov, A. Lazaro, and A. Barrado, "QZSI DC-DC converters in input-series output-parallel connection for distributed generation," in *Proc. Int. Symp. Power Electron. Electr. Drives, Autom. Motion*, Jun. 20–22, 2012, pp. 952–957.

[74] L. Pan, "L-Z-source inverter," *IEEE Trans. Power Electron.*, vol. 29, no. 12, pp. 6534–6543, Dec. 2014.

[75] J. J. Soon and K.-S. Low, "Sigma-Z-source inverters," *IET Power Electron.*, vol. 8, no. 5, pp. 715–723, 2015.

[76] M.-K. Nguyen, T.-V. Le, S.-J. Park, and Y.-C. Lim, "A class of quasi-switched boost inverters," *IEEE Trans. Ind. Electron.*, vol. 62, no. 3, pp. 1526–1536, Mar. 2015.

[77] A.-V. Ho, T.-W. Chun, and H.-G. Kim, "Extended boost active-switched-capacitor/switched-inductor quasi-Z-source inverters," *IEEE Trans. Power Electron.*, vol. 30, no. 10, pp. 5681–5690, Oct. 2015.

[78] B. Axelrod, Y. Berkovich, and A. Ioinovici, "Switched-capacitor/switched-inductor structures for getting transformerless hybrid DC–DC PWM converters," *IEEE Trans. Circuits Syst. I, Reg. Papers*, vol. 55, no. 2, pp. 687–696, Mar. 2008.

[79] T. Takiguchi and H. Koizumi, "Quasi-Z-source dc-dc converter with voltage-lift technique," in *Proc. IEEE 39th Annu. Conf. Ind. Electron. Soc.*, Nov. 10–13, 2013, pp. 1191–1196.

[80] W, Mo, P.-C. Loh, and F. Blaabjerg, "Asymmetrical Γ-source inverters," *IEEE Trans. Ind. Electron.*, vol. 61, no. 2, pp. 637–647, Feb. 2014.
[81] M.-K. Nguyen, Y.-C. Lim, and S.-J. Park, "Improved trans-Z-source inverter with continuous input current and boost inversion capability," *IEEE Trans. Power Electron.*, vol. 28, no. 10, pp. 4500–4510, Oct. 2013.
[82] M. Adamowicz, R. Strzelecki, F. Z. Peng, J. Guzinski, and H. A. Rub, "New type LCCT-Z-source inverters," in *Proc. 14th Eur. Conf. Power Electron. Appl.*, Aug. 30/Sep. 1, 2011, pp. 1–10.
[83] A. Blinov, D. Vinnikov, O. Husev, and A. Chub, "Experimental analysis of wide input voltage range qZS-derived push-pull DC/DC converter for PMSG-based wind turbines," in *Proc. PCIM Eur.*, May 14–16, 2013, pp. 1435–1444.
[84] T. Jalakas, I. Roasto, D. Vinnikov, and H. Agabus, "Novel power conditioning system for residential fuel cell power plants," in *Proc. IEEE 3rd Int. Symp. Power Electron. Distrib. Gener. Syst.*, Jun. 25–28, 2012, pp. 578–585.
[85] Q. T. Nha, C.-Y. Lin, M. M. Alam, Y.-K. Lo, and H.-J. Chiu, "Implementation of a single-stage quasi Z-source AC-DC power factor correction converter," in *Proc. Int. Conf. Anti-Counterfeiting, Secur. Identif.*, Aug. 24–26, 2012, pp. 1–5.

Andrii Chub (S'12) received the B.Sc. degree in electronics and the M.Sc. degree in electronic systems from Chernihiv State Technological University, Chernihiv, Ukraine, in 2008 and 2009, respectively. He is currently working toward the Ph.D. degree at the Power Electronics Research Group, Tallinn University of Technology, Tallinn, Estonia.

He is a Junior Researcher at the Department of Electrical Engineering, Tallinn University of Technology. He has coauthored more than 25 papers and one book chapter on power electronics and applications. His research interests include dc–dc converters, dc–ac inverters, impedance-source electric energy conversion technology, implementation of the new widebandgap semiconductors in power converters, and control of the renewable energy conversion systems.

Dmitri Vinnikov (M'07–SM'11) received the Dipl.Eng., M.Sc., and Dr. Sc. techn. degrees in electrical engineering from the Tallinn University of Technology, Tallinn, Estonia, in 1999, 2001, and 2005, respectively.

He is currently the Head at the Power Electronics Research Group, Department of Electrical Engineering, Tallinn University of Technology. He has authored more than 150 published papers on power converter design and development and is the holder of several patents and utility models in this field. His research interests include switch-mode power converters, modeling and simulation of power systems, applied design of power converters and control systems, and application and development of energy-storage systems.

Frede Blaabjerg (S'86–M'88–SM'97–F'03) received the Ph.D. degree from Aalborg University, Aalborg, Denmark, in 1992.

From 1987 to 1988, he was with ABB-Scandia, Randers, Denmark. He became an Assistant Professor in 1992, an Associate Professor in 1996, and a Full Professor of power electronics and drives in 1998. His current research interests include power electronics and its applications, such as in wind turbines, PV systems, reliability, harmonics, and adjustable speed drives.

Dr. Blaabjerg received 15 IEEE Prize Paper Awards, the IEEE PELS Distinguished Service Award in 2009, the EPE-PEMC Council Award in 2010, the IEEE William E. Newell Power Electronics Award 2014, and the Villum Kann Rasmussen Research Award in 2014. He was an Editor-in-Chief of the IEEE TRANSACTIONS ON POWER ELECTRONICS from 2006 to 2012. He was a Distinguished Lecturer for the IEEE Power Electronics Society from 2005 to 2007 and for the IEEE Industry Applications Society from 2010 to 2011. In 2014, he was nominated by Thomson Reuters to be between the most 250 cited researcher in engineering in the world.

Fang Zheng Peng (M'92–SM'96–F'05) received the B.S. degree in electrical engineering from Wuhan University, Wuhan, China, in 1983, and the M.S. and Ph.D. degrees in electrical engineering from the Nagaoka University of Technology, Nagaoka, Japan, in 1987 and 1990, respectively.

From 1990 to 1992, he was a Research Scientist with Toyo Electric Manufacturing Company, Ltd., Toyo, Japan, where he was involved in the research and development of active power filters, flexible ac transmission system (FACTS) applications, and motor drives. From 1992 to 1994, he was with the Tokyo Institute of Technology, Tokyo, as a Research Assistant Professor, where he initiated a multilevel inverter program for FACTS applications and a speed-sensorless vector control project. From 1994 to 1997, he was a Research Assistant Professor with the University of Tennessee, Knoxville, TN, USA. From 1994 to 2000, he was with the Oak Ridge National Laboratory, where from 1997 to 2000, he was the Lead (Principal) Scientist with the Power Electronics and Electric Machinery Research Center. Since 2000, he has been with Michigan State University, East Lansing, MI, USA, where he is currently a University Distinguished Professor at the Department of Electrical and Computer Engineering. He is the holder of more than 15 patents.

Dr. Peng received many awards including the IEEE/IAS IPCSD 2013 Gerald Kliman Innovator Award; the 2009 Best Paper Award in the IEEE TRANSACTIONS ON POWER ELECTRONICS; the 2011, 2010, 1996, and 1995 Prize Paper Award of Industrial Power Converter Committee in IEEE/IAS; the 1996 Advanced Technology Award of the Inventors Clubs of America, Inc., the International Hall of Fame; the 1991 First Prize Paper Award in the IEEE TRANSACTIONS ON INDUSTRY APPLICATIONS; and the 1990 Best Paper Award in the Transactions of the IEE of Japan, the Promotion Award of Electrical Academy. He was an IEEE TAB Awards and Recognition Committee Member and has served the IEEE Power Electronics Society in many capacities: the Chair of Technical Committee for Rectifiers and Inverters, an Associate Editor for the IEEE POWER ELECTRONICS TRANSACTIONS, the Region 1-6 Liaison, a Member-at-Large, the Awards Chair, and a Fellow Evaluation Committee Member.